

Multi-particle effects in non-equilibrium electron tunnelling and field emission

Andrei Komnik and Alexander O. Gogolin

Department of Mathematics, Imperial College, 180 Queen's Gate, London SW7 2BZ, United Kingdom

(Dated: October 30, 2018)

We investigate energy resolved electric current from various correlated host materials under out-of-equilibrium conditions. We find that, due to a combined effect of electron-electron interactions, non-equilibrium and multi-particle tunnelling, the energy resolved current is finite even above the Fermi edge of the host material. In most cases, the current density possesses a singularity at the Fermi level revealing novel manifestations of correlation effects in electron tunnelling. By means of the Keldysh non-equilibrium technique, the current density is calculated for one-dimensional interacting electron systems and for two-dimensional systems, both in the pure limit and in the presence of disorder. We then specialise to the field emission and provide a comprehensive theoretical study of this effect in carbon nanotubes.

PACS numbers: 03.65.X, 71.10.P, 73.63.F

I. INTRODUCTION

At the early stages of the development of the quantum theory it became clear that electron tunnelling processes are of fundamental importance for condensed matter physics [1]. Electron tunnelling became an essential concept in such fields as semiconductor physics, particle transport in mesoscopic physics, field emission, and many others. In a multitude of setups, tunnelling processes have attracted attention over decades and continue to do so.

For the purposes of this work, we shall visualise tunnelling events as taking place between a metallic host material and a lead material (another metal, a semiconductor, or indeed vacuum as in the field emission effect). The host and the lead are separated from each other by a substantial potential barrier. The lead is supposed to contain a detector measuring the current density. The presence of a finite current immediately implies that one is dealing with a non-equilibrium (steady-state) system. Apart from the total current, the energy resolved current $j(\omega)$, i. e. the amount of current in the energy window ω to $\omega+d\omega$, is an important characteristic of the tunnelling process. The total current J is then the integral of $j(\omega)$ over all energies. In the field emission (FE) setup, the energy resolved current have been measured for different emitters over some 30 years (see [2], and also references below). We shall therefore adopt the terminology of the Gadzuk and Plummer's review article, [2], and refer to $j(\omega)$ as the total energy distribution or TED. We are not aware of any direct measurements of TEDs in tunnelling contacts.

From the physical point of view, the most interesting aspect of the TED is the part of the spectrum above the Fermi edge, $\omega > E_F$. At the leading order in the tunnelling amplitude, $j(\omega)$ is simply proportional to tunnelling probability times the electron energy distribution function in the host, $n(\omega)$. The latter is identically zero (at zero temperature) above the Fermi edge due to the Luttinger theorem [3]. The high-energy tail is due to a combined effect of non-equilibrium, multi-particle tun-

nelling processes, and mutual electron-electron interactions in the host material (for non-equilibrium multi-particle effects *per se* are not sufficient to smear the Fermi surface [4]). So, we shall also refer to this high-energy tail of the energy resolved current distribution as 'secondary' current, 'primary' current being the one below the Fermi edge (i. e. the one which is proportional to the tunnelling probability). In the grand picture, the secondary current is akin to the Auger effect though it is, of course, a more complex phenomenon taking place not in an atom but in a fully interacting metallic host. Measurements of the secondary current (the trivial thermal broadening of the primary current being subtracted off) can thus provide a valuable source of information about the electronic correlations in the host [2, 5]. The effect was indeed first discovered experimentally – in FE measurements by Lea and Gomer [6]. Theoretical analysis of this phenomenon was done by Gadzuk and Plummer soon afterwards [7]. Following the pioneering paper by Fowler and Nordheim [8] these authors used the connection between the FE problem and the tunnelling problem and studied Boltzmann-like equations for the particle-hole balance in the low density approximation. To remove such restrictions and to put the theory on the modern footing, so that it becomes applicable to strongly-correlated emitters, we embark in this paper on investigating the issue by employing Keldysh diagram technique, appropriate for this non-equilibrium situation [9, 10]. This method allows us to consistently write down series in the tunnelling amplitude for all quantities of interest and for the TED in particular.

Our motivation is in fact two-fold. On one hand, we think that the secondary current phenomenon has not received sufficient attention of theorists. The physics of the interplay between non-equilibrium multi-particle tunnelling and electron correlations is worth a deeper study. In particular, we investigate in this paper what aspects of the electron correlations are responsible for the current above the Fermi edge and in what setups, other than the FE, such current can occur. On the other hand, since the original work [6, 7] there have been con-

siderable advances in the emitter technology. Perhaps the most important recent development is the usage of carbon nanotubes as field emitters. Carbon nanotubes display a remarkable array of electronic and mechanical properties and are of potential technological importance [11]. Electron transport in these systems has been thoroughly investigated. While single-wall nanotubes (SWNTs) exhibit one-dimensional (1D) Luttinger liquid (LL) type transport properties and are pretty well understood, the theory [12, 13, 14] and experiment being in agreement [15, 16], multi-wall nanotubes (MWNTs) are more complex systems subject to intensive current debate. MWNTs are composed from many (at least ten) concentric graphite shells. Current experiments on them are consistent with two-dimensional (2D) diffusion with characteristic weak localisation [17] features and zero-bias anomalies [18, 19, 20, 21]. What concerns us here is that, apart from other uses, carbon nanotubes are expected to act as field emitters in high-resolution displays and cathode tubes [22, 23]. While there have been several experimental investigations of the FE from carbon nanotubes (see [24] and the main text for more references), both from SWNTs and MWNTs, the relevant theory has been lacking. So, the second leg of our motivation is to discuss existing FE experiments on carbon nanotubes and make further theoretical predictions for these systems.

Having in mind applications to carbon nanotubes and taking into account the fact that FE usually occurs from a tip of the tube (both for SWNTs and MWNTs) we narrow the following considerations from a number of imaginable setups to an appropriate tip geometry. Apart from this restriction, we intent to advance in this paper a general discussion of non-equilibrium multi-particle tunnelling from strongly-correlated 1D and 2D hosts paying special attention to carbon nanotubes. Some of the results on 1D emitters (applicable to SWNTs) have been announced in our recent letter [5].

The paper is organised as follows. In the next Section we present some qualitative considerations concerning the physical nature of the TED. Section III contains general (model-independent) results. We identify the relevant Keldysh diagrams contributing to the TED above the Fermi edge and then perform a spectral analysis of the involved correlation functions. A simple application of the developed theory is contained in Section IV, where we treat an electron system with local interactions confined to the vicinity of the tunnelling point. In Section V we analyse the TED of particles tunnelling from LLs. In subsequent Sections VI and VII, the same problem is studied for correlated 2D electron systems, respectively in the pure limit and in the presence of a disorder potential. In Section VIII we specialise to the case of field emission from carbon nanotubes. Finally, in Section IX we discuss a more sophisticated two-stage tunnelling via a localised state. Summary and conclusions Section completes the paper.

II. PHYSICAL PICTURE

Before proceeding with calculations, let us elaborate on qualitative origins of the TED high-energy tails. The simplest setting to start with involves two noninteracting electrodes with a tunnelling contact between them, see Fig. 1. Applying a finite voltage leads to a nonzero current through the junction. Neglecting the charging effects and (for now) under the assumption of constant electron densities of states and transmission coefficient, the current is proportional to the applied voltage V . On the right side of the contact, where the chemical potential is supposed to be lower than on the left one, the current is carried by the tunnelled electrons. On the left side of the contact the current is carried by the holes moving in the opposite direction away from the contact. As long as the system is noninteracting, the TED of the electrons that tunnelled out is uniform in the window between E_F and $E_F - V$ and is zero outside (this is evident but can be confirmed by simple calculation in the spirit of [4], which we omit). From now on we set $e = 1$. E_F is the Fermi level of the left electrode.

This picture changes drastically if interactions between the electrons are switched on. We restrict our considerations to the case when only the left contact – the host – is correlated (see also discussion in the next Section). Then the difference between the actual energy distribution function in the lead and the noninteracting distribution function gives the TED of particles tunnelling out of the host. The holes left behind by electrons tunnelling out below the Fermi energy (‘primary’ electrons) experience scattering from the electron sea, thereby creating electron-hole pairs. Contrary to the problem of hot electron relaxation (see e. g. [25], and references therein), we are dealing here with a *flow* of hot holes in a steady state. Also, we are interested in a different object: the energy distribution functions rather than momentum distribution functions (the latter do, of course, have a non-zero tail above the Fermi momentum solely due to correlations, without a need to include tunnelling [26]). The emerging ‘secondary’ electrons can also be carried over to the lead by a successive tunnelling process, as shown in Fig. 1. This phenomenon can be regarded as condensed matter analogy of the Auger process known from the atomic physics. Since the energy of the holes, measured from the Fermi edge E_F , can not exceed V , the upper limit for the energy the secondary electrons can acquire in the electron-hole pair creation process is given by V as well. At higher orders in the tunnelling probability this threshold is increased so that the secondary electrons can, in fact, become more energetic than V . In this case they ought to be successively scattered either from another hot hole or from another hot electron. This is, however, a process of higher order not only in the tunnelling but also in the interaction. Therefore secondary electrons with energies between $(n - 1)V$ and nV emerge in the processes of $2n$ th order with respect to the tunnelling amplitude as well as the interaction constant.

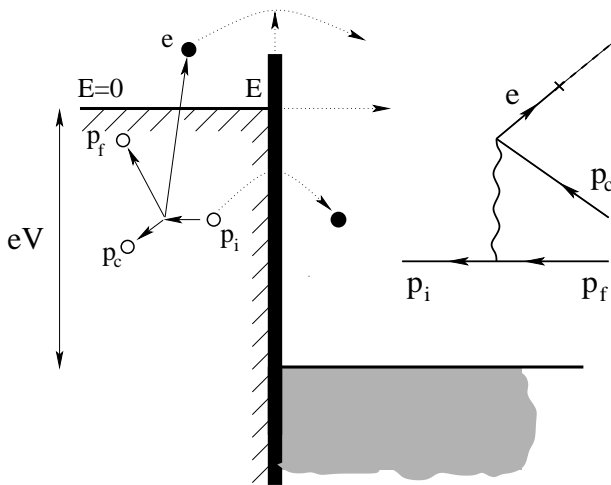


FIG. 1: Tunnelling junction biased by finite voltage V . The left electrode is the interacting one while the right one is uncorrelated. Tunnelling electrons with energies higher than E_F are due to hot hole (denoted by p_i) scattering with creation of electron-hole pairs $e - p_c$ (see inset).

Obviously, in equilibrium $V = 0$ all the high energy tails vanish, thereby restoring the Fermi edge in accordance with the Luttinger theorem. So, non-trivial interaction effects are encoded in the high-energy behaviour of the non-equilibrium TED.

Theoretically, the most interesting limiting case is the behaviour of the TED just above the Fermi edge, when certain universality can be expected. Out of the considerations of Ref. [7] a divergent TED emerged, with (simplifying matters) the singularity approximately of the form $j(\omega) \sim 1/(\omega - E_F)$. This turned out to be roughly consistent with measurements at the time [6]. As detailed in the following Sections, the present study supports the view that the limiting form of the TED strongly depends on the nature of the host material and the geometry of the setup (within a given material type though, some universality does set in, so for point-contacted LLs we find a power-law behaviour, etc.).

III. STATEMENT OF THE PROBLEM AND GENERAL RESULTS

We now formalise the problem by writing down the relevant tunnelling Hamiltonian:

$$H = H[c] + H[\psi] + \gamma [\psi^\dagger(0)c(0) + c^\dagger(0)\psi(0)] . \quad (1)$$

Here γ is the tunnelling amplitude and c and ψ are the annihilation operators for the electrons in the lead and in the host, respectively. The unperturbed part of the Hamiltonian $H_0 = H[c] + H[\psi]$ describes two decoupled electron systems at different chemical potentials $\mu_\psi - \mu_c = V > 0$.

A clarification on the following points is in order.

(i) As we only want to consider a tip geometry, we have explicitly assumed that the tunnelling occurs only locally at the location of the tip: $x = 0$. In reality, of course, there is a small area over which the tunnelling takes place (strictly speaking, a real-space integral is required in the tunnelling term in Eq.(1)). As this has no qualitative influence, we shall keep writing simple as long as we can. The locality assumption is natural for carbon nanotubes because of the very shape of these objects. It is however also justified for most bulk interfaces and field emitters where, because of the roughness of the surface and the pronounced exponential dependence of the penetration coefficient on the distance between the electrodes, the main contribution to the current comes from only few points between the electrodes.

(ii) Related to the above is the question of the energy (momentum) dependence of the tunnelling amplitude. In real systems it is energy dependent. So, for the FE setup the relevant energy scale is determined by a combination of the work function and the applied field. It is important to keep in mind, however, that as the tunnelling amplitude is a single electron property, regarding its energy dependence there is no special significance to the Fermi edge. Therefore, when addressing observables determined by scattering processes taking place close to the Fermi surface, it is quite safe to neglect the energy dependence of the tunnelling amplitude and replace it by a constant, γ (γ^2 being proportional to the transmission coefficient of the potential barrier at the Fermi energy: $\mathcal{D}(E_F)$.) In the literature on the subject the tunnelling term is often quoted in the momentum representation in the form $\gamma_{pk}\psi_p^\dagger c_k$ plus conjugate with some unspecified matrix elements γ_{pk} . We take the view that, for calculating quantities related to the Fermi surface, this would only complicate formulae without conceptual gain. There will be, however, instances in the following when the energy dependence of the tunnelling amplitude is important, like when there is a localised state or when we discuss generalisations of the Fowler–Nordheim relations for nanotubes. In these cases (Sections VIII and IX) we shall take the relevant energy dependence fully into account.

(iii) Throughout this paper we assume that the lead is non-interacting. Indeed one could not otherwise separate the effect of correlations occurring in the host from those occurring in the lead, which would seriously hamper meaningful interpretation of measurements on such systems. This assumption is justified for the FE setup, save for the Boersh effect, which is not believed to be important for carbon nanotubes (see [27] and [5]). For a general tunnelling junction setup it would not be correct to *a priori* neglect correlations in the lead. However, with care it is possible to realise a reasonable setup involving, for instance, a nanotube in contact with a low carrier density semiconductor or a quantum wire opening up into a higher dimensional lead preferably screened by a nearby gate (in fact most conductance measurements on quantum wires are nowadays interpreted in terms of

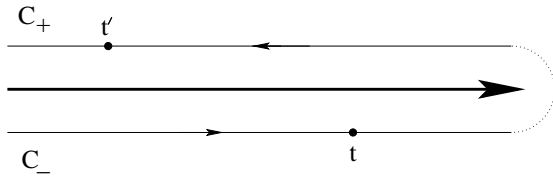


FIG. 2: Schematic representation of the Keldysh contour. The lower branch is time-ordered, while the upper branch is anti-time-ordered.

a junction with a non-interacting lead [28, 29]).

In the bulk of this paper we shall be investigating the secondary current $j(\omega > 0)$ (we set $E_F = 0$ from now on). It is a plausible statement that the secondary current should be proportional to the high-energy tail $n(\omega > 0)$ of the electron energy distribution function *inside* the emitter tip (calculated to all orders in the tunnelling amplitude). Indeed the latter quantity corresponds to the amount of electrons available for tunnelling at a given energy ω , while the proportionality factor contains (unessential) information about how these electrons are then carried over to the detector. In the first part of this Section we establish this statement.

Since we are dealing with non-equilibrium phenomena we resort to the Keldysh formalism. We denote by $G(x, x'; t - t')$ the generalised Green's function for electrons in the lead,

$$G(x, x'; t - t') = -i \langle T_C [c(x, t) c^\dagger(x', t')] S_C \rangle_0, \quad (2)$$

the Green's function in the host, g , being defined by an analogous formula. Here T_C stands for the ordering operation along the Keldysh contour, shown in Fig. 2, and x corresponds to a set of coordinates specifying the electron states in the lead. (It should be understood as a distance from the emitter tip plus possibly a transverse channel index which we suppress as it plays no important part in the following). The average in Eq. (2) is taken over the ground-states of the unperturbed Hamiltonian H_0 and the contour S_C -matrix is responsible for tunnelling events:

$$S_C = T_C \exp \left(-i\gamma \int_C dt [\psi^\dagger(t)c(t) + c^\dagger(t)\psi(t)] \right).$$

Note that because the system is not translationally invariant, all Green's functions depend on both coordinates. However, all functions still only depend on the time differences because the system is in steady state. The time integration in Eq. (2) is along the contour C . Keldysh disentanglement of the time variables results in expressions with integrations only along the real axis. Then, four different Green's functions emerge in accordance with four possibilities to arrange the times t and t' along the contour. This placement of the time variables is reflected in additional superscripts of the Green's functions. For instance, if the time t lies on the time-ordered

$$- \text{---} = \text{- - - -} + \text{---} \bullet \text{---}$$

FIG. 3: Schematic representation of the equation (4). Solid line denotes the electron's Green's function of the lead and the dashed ones stand for particles in the host. Thick lines they correspond to exact Green's functions to all orders in tunnelling and interactions while thin lines represent Green's functions with tunnelling neglected.

part of the contour and t' on the anti-time-ordered one, see Fig. 2, evaluation of Eq. (2) at the zeroth order in the tunnelling (indicated by a subscript 0) yields:

$$\begin{aligned} G_0^{-+}(x, x'; t - t') &= -i \langle T_C [c(x, t) c^\dagger(x', t')] \rangle_0 \\ &= i \langle c^\dagger(x', t') c(x, t) \rangle_0. \end{aligned}$$

Its counterpart with an interchanged orientation of time variables (t on the C_+ and t' on the C_-) is

$$G_0^{+-}(x, x'; t - t') = -i \langle c(x, t) c^\dagger(x', t') \rangle_0.$$

Green's function in which both time variables lie on the same side of the contour are the usual time-ordered and anti-time-ordered ones:

$$\begin{aligned} G_0^{--}(x, x'; t - t') &= -i \langle T [c(x, t) c^\dagger(x', t')] \rangle_0, \\ G_0^{++}(x, x'; t - t') &= -i \langle \tilde{T} [c(x, t) c^\dagger(x', t')] \rangle_0, \end{aligned}$$

where \tilde{T} denotes the anti-time-ordering operation.

The local electron energy distribution function $N(x, \omega)$ in the lead, which we shall also call TED by abuse of terminology, is given by the defining relation with one of the Keldysh Green's functions (see e. g. [10]):

$$N(x, \omega) = -i G^{-+}(x, x; \omega). \quad (3)$$

The lead being non-interacting, the TED of the tunnelling particles is, up to a pre-factor, given by above Green's function after subtracting off the equilibrium distribution function. Indeed, by examining the perturbative expansion in the tunnelling amplitude γ and keeping in mind the fact that there is no correlations in the lead, one can easily establish the following important identity,

$$\begin{aligned} G(x, x'; t - t') &= G_0(x, x'; t - t') \\ &+ \gamma^2 \int_C \int_C dt'' dt''' G_0(x, 0; t - t'') g(0, 0; t'' - t''') \\ &\times G_0(0, x'; t''' - t'). \end{aligned} \quad (4)$$

The corresponding diagram is shown in Fig. 3. The function $g(0, 0; t - t')$ appearing in this relation is the exact one, so the formula is valid for arbitrary interactions in the host and to all orders in the tunnelling amplitude.

By disentangling the Keldysh indices and changing over to the energy representation, we extract the Green's function of interest from the general expression, (4),

$$\begin{aligned} G^{-+}(x, x'; \omega) &= G_0^{-+}(x, x'; \omega) \\ &+ \gamma^2 \sum_{i,j=\pm} (ij) G_0^{-i}(x, 0; \omega) g^{ij}(0, 0; \omega) G_0^{j+}(0, x'; \omega). \end{aligned} \quad (5)$$

Plugging this expression into Eq. (3) one obtains the complete TED at all energies. Let us take a closer look at this relation. All terms on the right-hand-side, apart of the one with $(i, j) = (-, +)$, contain the unperturbed G_0^{-+} function. The latter is, in turn, proportional to the TED in equilibrium. Therefore, no matter what the Green's functions of the interacting fermions look like, all these contributions represent the TED below the Fermi energy (where the first term is the dominant contribution). The term in Eq. (5) with $(i, j) = (-, +)$ is not constrained in such way and can, in principle, contribute above the Fermi edge. Therefore the high-energy part of the TED is given by

$$\begin{aligned} N_>(x; \omega) &= -i\Theta(\omega)G^{-+}(x, x; \omega) \\ &= -\gamma^2 G_0^{-}(x, 0; \omega)g_{>}^{-+}(0, 0; \omega)G_0^{++}(0, x; \omega), \end{aligned} \quad (6)$$

where $\Theta(\omega)$ is the Heaviside step function and $g_{>}^{-+}(0, 0; \omega)$ stands for the high energy part of the corresponding Green's function.

Similar properties can be established for the energy resolved current $j(\omega)$, when we have

$$j(\omega) = \frac{1}{\pi} \int dk v_k N(k; \omega)$$

where v_k is the velocity of the particle with wave number k . Making use of Eqs. (3) and (5) for the high-energy part of the current one obtains,

$$\begin{aligned} j_>(\omega) &= -i\frac{\gamma^2}{\pi} g_{>}^{-+}(0, 0; \omega) \\ &\times \int dk k \int d(x - x') e^{ik(x-x')} \\ &\times [G_0^{-}(x, 0; \omega)G_0^{++}(0, x'; \omega)], \end{aligned} \quad (7)$$

where the product in brackets is actually translationally invariant (only depends on $x - x'$), reflecting the fact that the excess particles only travel in one direction, away from the contact, in the (non-interacting) lead.

We now observe that both Eq. (6) and Eq. (7) are proportional to the high-energy part of the TED of particles at the tip of the interacting host,

$$n_>(\omega) = -ig_{>}^{-+}(0, 0; \omega), \quad (8)$$

thereby proving the statement put forward at the beginning of this Section. We stress again that $n_>(\omega)$ is supposed to be exact both with respect to the interaction and the tunnelling. Indeed, as one can easily see, this quantity is zero for a noninteracting system, even if tunnelling is taken into account to all orders. It is still zero for interacting hosts if tunnelling is neglected or if the system is in equilibrium (Luttinger theorem). Situation changes dramatically in the case of an interacting host, finite tunnelling and finite bias voltage. In the rest of this Section we shall explore what statements can be made about the TED without assuming a concrete model for the host material (other than that there is a two-body interaction present).

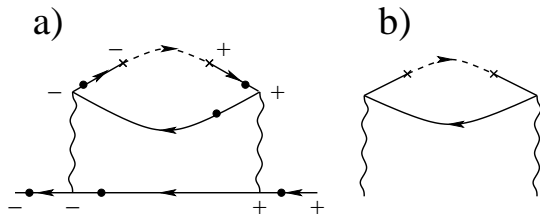


FIG. 4: a) The only second order diagram contributing to the TED above the Fermi energy. Solid lines correspond to host electrons and the dashed one to those in the lead while crosses denote the tunnelling vertices. Wiggly lines represent interactions. b) This diagram has to be inserted into a) at points denoted by circles in order to obtain high-order diagram for the TED.

As mentioned in the Introduction, there is a scattering process that allows for creation of electrons above the Fermi energy. Let us start with perturbative analysis. At the second order in the interaction, the corresponding diagram for the Green's function can be constructed by annihilating the particles in the same way they were created. This essentially converts the scattering amplitude for a given process into the corresponding probability. The result is shown in Fig. 4 a). Now we need to establish the way the vertices can be decorated with the Keldysh indices. Trivially the outmost points should have index $-$ on the outward leg and $+$ on the inward leg in accordance with the type of function $(-+)$ we are calculating. Furthermore, there is only one possibility to assign indices to interaction vertices. In order to obtain a contribution above the Fermi energy the inward Green's function should be of $++$ or anti-time ordered type while the outward one has to carry $--$ indices, because all other possibilities contain at least one G_0^{-+} factor which forces the diagram to vanish above E_F . We are left with two cross vertices of the inserted Green's function. Since we do not have *a priori* knowledge about them, we have checked all possibilities explicitly. It turns out that the only possibility is to insert the function G_0^{+-} because in all other cases the diagram vanishes for $\omega > 0$. Hence the only second-order diagram contributing to the TED above the Fermi energy is the one shown in Fig. 4 a).

Let us now consider all orders in the interaction but remain at the second order in the tunnelling amplitude thereby also formally justifying the above choice of the Keldysh indices. The way to proceed is to analyse the relevant Green's functions in the Lehmann-type spectral representation. In the time domain the local (tip) Green's function of interest $g^{-+}(t_1, t_2)$ is given by

$$g^{-+}(t_1, t_2) = i\langle \psi^\dagger(t_2)\psi(t_1) \rangle = -i\langle T_C[\psi(t_1^-)\psi^\dagger(t_2^+)] \rangle,$$

where the superscripts indicate that the time variables t_1 and t_2 lie on the time-ordered (T) and anti-time-ordered (\tilde{T}) parts of the Keldysh contour, respectively. Performing the straightforward S -matrix expansion in powers of the tunnelling amplitude γ one obtains at the lowest non-

vanishing order (second order in γ):

$$\begin{aligned} \delta g^{-+}(t_2, t_1) &= \gamma^2 \int dt_3 dt_4 \sum_{ij=\pm} \mathcal{K}_{ij}^{-+}(t_2, t_1; t_3, t_4) \\ &\times G^{ij}(t_3, t_4), \end{aligned} \quad (9)$$

where $\mathcal{K}_{ij}^{-+}(t_2, t_1; t_3, t_4)$ are the following four-point correlation functions:

$$\begin{aligned} \mathcal{K}_{+-}^{-+}(t_1, t_2; t_3, t_4) &= \langle \tilde{T}[\psi^\dagger(t_2)\psi^\dagger(t_3)]T[\psi(t_1)\psi(t_4)] \rangle_0, \\ \mathcal{K}_{-+}^{-+}(t_1, t_2; t_3, t_4) &= \langle \tilde{T}[\psi(t_4)\psi^\dagger(t_2)]T[\psi(t_1)\psi^\dagger(t_3)] \rangle_0, \\ \mathcal{K}_{--}^{-+}(t_1, t_2; t_3, t_4) &= \langle \psi^\dagger(t_2)T[\psi(t_1)\psi^\dagger(t_3)\psi(t_4)] \rangle_0, \\ \mathcal{K}_{++}^{-+}(t_1, t_2; t_3, t_4) &= \langle \tilde{T}[\psi^\dagger(t_2)\psi^\dagger(t_3)\psi^\dagger(t_4)]\psi(t_1) \rangle_0 \end{aligned} \quad (10)$$

We shall first find the spectral representation of the term containing \mathcal{K}_{+-}^{-+} ,

$$\begin{aligned} \delta^{(1)} g^{-+}(t_1, t_2) &= \gamma^2 \int \frac{d\epsilon}{2\pi} G^{+-}(\epsilon) \\ &\times \int dt_3 dt_4 e^{-i\epsilon(t_3-t_4)} \mathcal{K}_{+-}^{-+}(t_1, t_2; t_3, t_4) \\ &= -i\gamma^2 \int_{-V}^{\infty} d\epsilon \rho_c(\epsilon) P_{+-}^{-+}(t_1, t_2; \epsilon), \end{aligned} \quad (11)$$

where we have used the bare $-+$ Green's function in the lead,

$$G_0^{+-}(\epsilon) = -i2\pi\Theta(\epsilon + V)\rho_c(\epsilon), \quad (12)$$

containing the local density of states $\rho_c(\epsilon)$ in the lead. Partial Fourier transform of the correlation function appearing in the above formula is defined by

$$P_{+-}^{-+}(t_1, t_2; \epsilon) = \int dt_3 dt_4 e^{-i\epsilon(t_3-t_4)} \mathcal{K}_{+-}^{-+}(t_1, t_2; t_3, t_4).$$

According to definition (10), this correlation function contains two different time orderings. Writing them down explicitly and inserting between every two ψ operators a complete set of exact states, it is possible to perform all time integrations. This procedure is a straightforward generalisation of the standard one for the equilibrium case [26]. The result is

$$P_{+-}^{-+}(t_1, t_2; \epsilon) = \sum_{\mu} e^{-i(E_{\mu}+\epsilon)(t_1-t_2)} |\mathcal{B}_{\mu}^{(1)}(\epsilon)|^2, \quad (13)$$

with $\mathcal{B}_{\mu}^{(1)}(\epsilon)$ defined by

$$\mathcal{B}_{\mu}^{(1)}(\epsilon) = \sum_{\nu} a_{\mu\nu} a_{\nu 0} \left[\frac{1}{E_{\mu} - E_{\nu} + \epsilon + i0} + \frac{1}{E_{\nu} + \epsilon - i0} \right],$$

where Greek indices count all possible excited states of the system with energies $E_{\nu, \lambda, \mu}$ and $a_{\mu\nu}$ stand for matrix elements of the operator ψ , $a_{\mu\nu} = \langle \mu | \psi | \nu \rangle$. In order to obtain the actual correction to the TED we plug the two last equations back into Eq. (11) and compute the

Fourier transform of the latter with respect to the time difference $t_1 - t_2$,

$$\begin{aligned} \delta n^{(1)}(\omega) &= -i \int d(t_1 - t_2) e^{i\omega(t_1-t_2)} \delta^{(1)} g^{-+}(t_1, t_2) \\ &= -2\pi\gamma^2 \sum_{\mu} \Theta(V - E_{\mu} - \omega) |\mathcal{B}_{\mu}^{(1)}(-V)|^2. \end{aligned}$$

Obviously, all E_{μ} 's are larger than the ground state energy E_0 (which we have set to zero). Therefore the upper boundary for ω is given by V .

The remaining three terms in Eq. (9) can be treated in a similar manner. Repeating steps leading to (13), we obtain for the term containing the second four-point correlation function in Eq. (10):

$$P_{-+}^{-+}(t_1, t_2; \epsilon) = \sum_{\mu} e^{i(E_{\mu}-\epsilon)(t_1-t_2)} |\mathcal{B}_{\mu}^{(2)}(\epsilon)|^2,$$

with

$$\mathcal{B}_{\mu}^{(2)}(\epsilon) = \sum_{\nu} \left[\frac{a_{0\mu} a_{\mu\nu}^*}{E_{\mu} - \epsilon + i0} + \frac{a_{0\mu}^* a_{\mu\nu}}{E_{\nu} - E_{\mu} - \epsilon - i0} \right],$$

the corresponding contribution to the TED being

$$\delta^{(2)} n(\omega) = 2\pi\gamma^2 \sum_{\mu} \Theta(-V - E_{\mu} - \omega) |\mathcal{B}_{\mu}^{(2)}(V)|^2. \quad (14)$$

Contrary to Eq. (14), this term is bounded by $-V$ from above and hence does not contribute to the high-energy part of the TED. One can use an even simpler argument in order to show that the last two four-point correlation functions in (10) do not contribute above the Fermi edge either. By inserting only one complete set of states between the time-ordered operators (i. e. at the break of the time-ordering) one obtains (for simplicity we set $t_1 = 0$)

$$\begin{aligned} P_{--}^{-+}(0, t_2; \epsilon) &= \int \int dt_3 dt_4 e^{-i\epsilon(t_3-t_4)} \\ &\times \sum_{\nu} a_{0\nu}^* e^{-iE_{\nu}t_2} \langle \nu | T[\psi(0)\psi^\dagger(t_3)\psi(t_4)] | 0 \rangle \end{aligned}$$

for the third term. The corresponding correction to the TED is then given by

$$\begin{aligned} \delta^{(3)} n(\omega) &= i\gamma^2 \sum_{\nu} a_{0\nu}^* \delta(-E_{\nu} - \omega) \int d\epsilon G_0^{--}(\epsilon) \\ &\times \int dt_3 dt_4 \langle \nu | T[\psi(0)\psi^\dagger(t_3)\psi(t_4)] | 0 \rangle. \end{aligned}$$

Since all E_{ν} 's are always positive this expression is nonzero only for negative energies $\omega < 0$. The same is true for the last four-point correlation function \mathcal{K}_{++}^{-+} .

The above approach is quite general (i. e. valid for all kinds of interacting host materials) but it is also inconclusive in the sense that the actual energy dependence of the TED is determined by spectral weights encoded in the structure of matrix elements $a_{\mu\nu}$ that is different

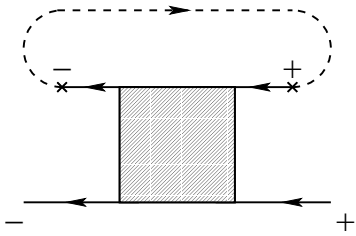


FIG. 5: Generic diagram giving contributing to the TED above the Fermi energy. The four-point correlation function $\mathcal{K}_{+-}^{-+}(t_1, t_2; t_3, t_4)$ is represented by the shaded square.

for different hosts. One positive result of the spectral method, however, is that we have identified the Keldysh four-point correlation function responsible for the secondary current effect: \mathcal{K}_{+-}^{-+} , see Fig. 5. For some models we shall calculate this correlation function exactly to all orders in the interaction, for other models we'll resort to perturbative expansions: note that diagram a) of Fig. 4 is a special case (second-order expansion) of the general Fig. 5 term.

Let us conclude the present Section by making one more observation of a general character. Returning back to the real time representation of the lead Green's function (12) and doing simple manipulations with the time integrations, we arrive at the alternative representation for the TED:

$$n_{>}(\omega) = -2i\gamma^2 \int_{-\infty}^{\infty} dt \frac{e^{i(\omega-V)t}}{t+i\alpha} \int_{-\infty}^{\infty} d\tau_1 \int_{-\infty}^{\infty} d\tau_2 e^{i\omega(\tau_1+\tau_2)} \times \langle \tilde{T}[\psi(\tau_1)\psi(0)]T[\psi(t+\tau_1)\psi(t+\tau_1+\tau_2)] \rangle_0, \quad (15)$$

where α stands for the short-time (high-energy) cutoff inversely proportional to the conductance band-width D . For the sake of simplicity, we have assumed a constant density of states in the lead but this assumption is not crucial. We now observe that if the T -ordering operation

$$\mathcal{R}(\tau_1, 0; t + \tau_1, t + \tau_1 + \tau_2) = (1 + e^{-i\varphi(\tau_1)})(1 + e^{-i\varphi(-\tau_2)}) \langle \psi^\dagger(\tau_1)\psi^\dagger(0)\psi(t + \tau_1)\psi(t + \tau_1 + \tau_2) \rangle \quad (20)$$

from which formula it is clear that the expansion of $n_{>}(\omega)$ in the interaction constant starts (at least) at the second order. In the next Section we present two models where such braiding relations exist.

In the following four Sections we apply the formalism developed here to various physical systems.

in the above formula were dropped, the expression would vanish. Indeed, inserting some complete sets one finds that then the integrand in the above, proportional to

$$\sim \langle 0|\psi(t + \tau_1)|\nu\rangle\langle\nu|\psi(t + \tau_1 + \tau_2)|0\rangle \sim e^{iE_\nu\tau_2}, \quad (16)$$

becomes an analytic function of the time variable τ_2 in the upper half plane and hence has vanishing Fourier transform for $\omega > 0$. By re-arranging time integrations in a different way, one can easily show that the same statement is true about the \tilde{T} -ordering operation. Subtracting off the unordered correlation function we arrive at the following remarkable representation for the TED:

$$n_{>}(\omega) = -2i\gamma^2 \int_{-\infty}^{\infty} dt \frac{e^{i(\omega-V)t}}{t+i\alpha} \int_0^{\infty} d\tau_1 \int_0^{\infty} d\tau_2 e^{i\omega(\tau_1+\tau_2)} \times \mathcal{R}(\tau_1, 0; t + \tau_1, t + \tau_1 + \tau_2), \quad (17)$$

with

$$\mathcal{R}(t_1, t_2; t_3, t_4) = \langle \{\psi^\dagger(t_1), \psi^\dagger(t_2)\} \{ \psi(t_3), \psi(t_4) \} \rangle, \quad (18)$$

where $\{.,.\}$ stands for the anti-commutator. The advantage of this representation is that it is explicitly vanishing in the non-interacting case as the field operators are then anti-commuting at all times. The latter does not take place in interacting systems. Generally, anti-commuting interacting Fermi operators at different times would result in a complicated object. However, there are systems for which the so-called *braiding relations* hold:

$$\psi(t_1)\psi(t_2) = e^{i\varphi(t_1-t_2)}\psi(t_2)\psi(t_1). \quad (19)$$

The exact shape of the phase function $\varphi(t)$ depends on the system in question but it is usually proportional to the interaction constant. The braiding relation reflects the time evolution of an anti-commutators in particular models and can be used to simplify (18) to

IV. MODELS WITH LOCAL INTERACTIONS

We start with the simplest (toy) model we could think of: the interactions are only present at one point - the tip of the emitter. The host Hamiltonian entering Eq. (1) is then of the form

$$H[\psi] = H_0[\psi] + H_i[\psi] \quad (21)$$

with the Hubbard on-site repulsion for the interaction term

$$H_i = U_0 \psi_{\uparrow}^{\dagger}(0) \psi_{\downarrow}^{\dagger}(0) \psi_{\downarrow}(0) \psi_{\uparrow}(0). \quad (22)$$

We take a half-infinite electron system with linear dispersion relation for the left electrode

$$H_0[\psi] = -i \sum_s \int_0^{\infty} dx \left[\psi_{sR}^{\dagger}(x) \partial_x \psi_{sR}(x) - \psi_{sL}^{\dagger}(x) \partial_x \psi_{sL}(x) \right],$$

and the same for the lead (but, of course, at chemical potential of $-V$). Here $\psi_{sR(L)}$ stands for the annihilation operator of the right(left)-moving electron species with spin s . To simplify the formulae we have set $\hbar v_F = 1$.

At first sight such model seems unphysical. However, it can be regarded as a special case of a correlated quantum dot contacted by two noninteracting electrodes, see e. g. Ref. [30], where the contact to one of them is nearly perfect while the contact to the other one is weak. One should then decorate the electron field operator with a tunnelling channel (transverse quantisation) index. Its presence does not affect qualitative results, so we drop the channel index in this Section.

For the half-infinite host, the bare Green's functions have image structure of the form

$$g_{s0}(x, x'; \omega) = g_0(x - x'; \omega) - g_0(x + x'; \omega), \quad (23)$$

and are diagonal and $s \rightarrow -s$ symmetric in the spin space. The Green's functions appearing on the right-hand-side in the above formula are the translationally invariant (bulk) ones for the corresponding spinless infinite system. The simplest Green's functions are the retarded and advanced ones,

$$g_0^R(x; \omega) = [g_0^A(x; \omega)]^* = -i e^{i(k_F + \omega)|x|} \quad (24)$$

to which the diagonal Keldysh functions are related via

$$g_0^{--}(x; \omega) = \Theta(\omega) g_0^R(x; \omega) + \Theta(-\omega) g_0^A(x; \omega) \quad (25)$$

and $g_0^{++}(x; \omega) = -[g_0^{--}(x; \omega)]^*$, while the off-diagonal Keldysh functions are:

$$g_0^{+(-+)}(x; \omega) = i 2 \Theta(\pm \omega) \cos \left[(k_F + \omega)x \right].$$

Plugging these expressions into Eq. (23) one obtains all Keldysh components for the half-infinite system. However, using them directly to evaluate $g_{s>}^{-+}(0, 0; \omega)$ for electrons with spin orientation s causes a technical problem as at the origin all wave functions of the half-infinite system vanish and so do the correlation functions. The reason for that is the open boundary condition imposed on the wave functions. Therefore we are in need of a regularisation. We now assume that the underlying lattice model has a lattice constant a_0 so that the tunnelling occurs between points with the spatial coordinate $x < a_0$

in the left subsystem as well as in the right one. Obviously, such regularisation does not influence the physics but only creates some non-universal numerical factors in the TED. In this regularisation all zeros in Eq. (6) are understood to be substituted by a_0 . Suppressing this argument in the formulas, we obtain the following expression for the second-order correction to the local (tip) Green's function (diagram Fig. 4 with an appropriate arrangement of the spin indices):

$$\begin{aligned} g_{s>}^{-+}(\omega) &= -\gamma^2 4 U_0^2 \Theta(\omega) g_0^{++}(\omega) g_0^{--}(\omega) \\ &\times \int d\epsilon_1 d\epsilon_2 g_0^{-+}(\omega - \epsilon_1) \\ &\times g_0^{-+}(\epsilon_1 + \epsilon_2) g_0^{--}(\epsilon_2) g_0^{++}(\epsilon_2) G_0^{+-}(\epsilon_2) \end{aligned} \quad (26)$$

where the local Green's functions in the lead (G 's) are understood to be the same as in the host but with energy measured from $-V$. To evaluate this diagram, it is useful to remember that

$$g_0^{++}(\omega) g_0^{--}(\omega) = -|g_0^R(\omega)|^2 = -4 \sin^2 [(k_F + \omega)a_0].$$

As we restrict our considerations to energy scales much smaller than the Fermi energy, we can regard these products essentially constant. The same is justified for other Green's functions except, of course, the step functions appearing in front of the off-diagonal Keldysh functions. Then, calculating energy integrals in Eq. (26), we obtain the following result for the TED:

$$n_{s>}(\omega) = -i g_{s>}^{-+}(\omega) = C_0 \gamma^2 U_0^2 \Theta(\omega) \Theta(V - \omega) (\omega - V)^2 / 2$$

(with the non-universal constant $C_0 = 4^5 \sin^{10}(k_F a_0)$).

Note that in accordance with the discussion in Section II no particles can have energy exceeding V at the second order in the interaction constant. Such particles, however, appear if one takes into account processes of higher order. The corresponding diagrams can easily be constructed, see Fig. 4. So, at the fourth order in the Hubbard U we found

$$g_{s>}^{-+}(\omega) = i C_0' \gamma^4 U_0^4 \Theta(\omega) \Theta(2V - \omega) (\omega - 2V)^4 / 24$$

(C_0' is again a non-universal numerical pre-factor). It is not difficult to calculate the particle spectrum for arbitrary ω . In the energy window between $V(n-1)$ and Vn ($n = 1, 2, \dots$) it is dominated by the term of the order $[\gamma U_0]^{2n}$ and shows $(nV - \omega)^{2n}$ decay.

Another interesting local model is the local phonon model, where the electron density operator is coupled to a local oscillator at the tip $x = 0$. In the chiral formulation the Hamiltonian of the problem is

$$\begin{aligned} H &= i \int dx \psi^{\dagger}(x) \partial_x \psi(x) + \Omega b^{\dagger} b \\ &+ \lambda \psi^{\dagger}(0) \psi(0) (b^{\dagger} + b) \end{aligned} \quad (27)$$

where b^{\dagger} and b are the creation and annihilation operators of the local phonon. The chirality of fermions takes

care of the reflecting boundary condition at the origin (see e. g. Ref. [31]) where the tunnelling processes take place. In the anti-adiabatic approximation (justified for high-frequency phonons, $\Omega \gg \lambda/a_0$), this Hamiltonian can be solved via the Fröhlich transformation [32]

$$H' = e^Q H e^{-Q}, \quad (28)$$

with

$$Q = \frac{\lambda}{\Omega} \psi^\dagger(0) \psi(0) (b^\dagger - b). \quad (29)$$

Simple transformations of the field operators, which we omit here, show that braiding relations are satisfied for this particular model and the braiding phase φ defined in Eq. (19) is equal to:

$$\varphi(t) = \pi + \frac{1}{2} \left(\frac{\lambda}{\Omega a_0} \right)^2 \sin[\Omega t]. \quad (30)$$

Using this result when evaluating Eqs. (15) and (18) we obtain for the TED:

$$n_{>}(\omega) = -2i\gamma^2 \int_{-\infty}^{\infty} dt \frac{e^{i(\omega-V)t}}{(t+i\alpha)^2} \int_0^{\infty} d\tau_1 \int_0^{\infty} d\tau_2 e^{i\omega(\tau_1+\tau_2)} (1 - e^{i(\lambda/\Omega a_0)^2 \sin[\Omega\tau_1]/2}) (1 - e^{-i(\lambda/\Omega a_0)^2 \sin[\Omega\tau_2]/2})$$

$$\times \frac{\tau_1 \tau_2}{(\tau_1 + \tau_2 + t + i\alpha)(\tau_1 + t + i\alpha)(\tau_2 + t + i\alpha)}.$$

Expanding in powers of $\lambda/\Omega a_0$ the evaluation of these integrals yields the main contribution to the TED of the form

$$n_{>}(\omega) \approx \frac{\pi\gamma^2}{2} \left(\frac{\lambda}{\Omega a_0} \right)^4 \Theta(V - \omega) \frac{\omega(V - \omega)}{\Omega^2 - \omega^2}. \quad (31)$$

As expected, the emerging spectrum has a resonant character having a sharp pole at the oscillator frequency Ω . Under appropriate conditions, the Fröhlich transformation can also be used for solving the bulk electron-phonon interaction where the braiding relations still persist. We shall not pursue this issue further in this paper.

V. LUTTINGER LIQUID MODEL

Staying with 1D hosts, we now move on to the next level of difficulty and discuss the bulk interactions. The

simplest model here is the spinless Luttinger liquid model [33]. Subject to minor modifications (see below) the LL results will also be applicable to quantum wires and SWNTs. The interacting term in the host Hamiltonian then is

$$H_i = \int dx dy \psi^\dagger(x) \psi^\dagger(y) U(x - y) \psi(y) \psi(x). \quad (32)$$

where $U(x)$ is the interaction potential.

Although this model can be exactly solved, it is instructive to start with the perturbative expansion. Diagram a) in Fig. 4 still represents the only non-vanishing contribution to the TED above the Fermi edge. Compared to Eq. (26), the analytic expression for this diagram is slightly more complicated since all participating Green's functions acquire spatial dependence. Assuming local interaction, $U(x - y) \rightarrow U_0 \delta(x - y)$, we write

$$g_{>}^{-+}(\omega) = -\gamma^2 U_0^2 \Theta(\omega) \int_{a_0}^{\infty} dx_1 dx_2 g_0^{++}(x_2, a_0; \omega) g_0^{--}(a_0, x_1; \omega) \int d\epsilon_1 d\epsilon_2 g_0^{-+}(x_1, x_2; \omega - \epsilon_1)$$

$$\times g_0^{-+}(x_1, x_2; \epsilon_1 + \epsilon_2) g_0^{--}(x_1, a_0; \epsilon_2) g_0^{++}(a_0, x_2; \epsilon_2) G_0^{+-}(a_0, a_0; \epsilon_2). \quad (33)$$

We use the same regularisation as in Section IV (that is why the lower boundary of the x -integration is the lattice constant a_0). Substituting the expressions for the corresponding bare Green's functions into this formula one obtains the following result:

$$g_{>}^{-+}(\omega) = i\gamma^2 U_0^2 8C_0 \Theta(\omega) \Theta(V - \omega) \int_{\omega}^V d\epsilon_1 \int_{-V}^{-\epsilon_1} d\epsilon_2 |H(\epsilon_1, \epsilon_2, \omega)|^2, \quad (34)$$

where C_0 is a non-universal numerical constant and the function H is defined as

$$H(\epsilon_1, \epsilon_2, \omega) = \frac{1}{2} \int_0^{\infty} dx e^{i(\omega - \epsilon_2)x} \cos[(2\epsilon_1 + \epsilon_2 - \omega)x] = -\frac{1}{4i} \frac{\epsilon_2 - \omega}{\epsilon_1(\epsilon_1 + \epsilon_2 - \omega)}.$$

We are ignoring terms containing rapidly oscillating integrands which are negligible on energy scales much smaller than E_F .

Performing the last energy integrals we obtain for the TED above the Fermi edge

$$n_{>}(\omega) = \gamma^2 U_0^2 \Theta(\omega) \Theta(V - \omega) C_0 \left\{ \frac{V - \omega}{\omega} + F_0 \left(\frac{\omega}{V} \right) \right\},$$

where $F_0(x)$ is a function regular at $x = 0$ and vanishing for $x > 1$. While the TED vanishes smoothly in the vicinity of $\omega = V$, there is a sharp singularity towards the Fermi edge.

Since the Luttinger liquid model is solvable for arbitrary interaction strength, [33], it is possible to go beyond the perturbative expansion. In particular, the four-point correlation function in Eq. (15) can be calculated exactly. We remind the reader that the system under consideration is a half-infinite spinless LL with an open boundary across which tunnelling processes occur. Using the standard bosonization scheme for open boundary LLs (technical details can be found in the literature, see [31, 34]), we write

$$\psi(x = 0, t) = (2\pi a_0)^{-1/2} \exp[i\phi(x = 0, t)/\sqrt{g}] \quad (35)$$

where g is the LL parameter, defined by $g = (1 +$

$4U_0/\pi)^{-1/2}$. The Gaussian chiral Bose field $\phi(x, t)$ has been rescaled and is governed by the LL Hamiltonian

$$H_{LL}[\phi] = \frac{1}{4\pi} \int_{-L}^L dx (\partial_x \phi)^2. \quad (36)$$

The Bose field is periodic in $2L$, where L is the system size. In order to obtain the correct analytic properties of correlation functions we first work with a system of a finite length L , which makes the energy quantisation equal to $\epsilon_0 = \pi/L$, and then send L to infinity. Using representation (35) we obtain the four-point correlation function in question:

$$\begin{aligned} \mathcal{K}_{+-}^-(t_1, t_2; t_3, t_4) &= (2\pi b)^{-2} \text{sgn}(t_2 - t_3) \text{sgn}(t_1 - t_4) \\ &\times \left[\frac{F(|t_2 - t_3|) F(|t_1 - t_4|) F^2(0)}{F(t_2 - t_1) F(t_2 - t_4) F(t_3 - t_1) F(t_3 - t_4)} \right]^{1/g}, \end{aligned} \quad (37)$$

where the function $F(t)$ is defined by

$$F(t) = 1 - e^{i\epsilon_0(t+i\delta)}.$$

In the thermodynamic limit $L \rightarrow \infty$, we expand Eq. (37) in powers of ϵ_0 . Then Eq. (15) can be brought into the following form

$$\begin{aligned} n(\omega) &= -2i\gamma^2 e^{-i\pi/g} \cos^2(\pi/2g) \int dt \frac{e^{i(\omega-V)}}{(-t - i\alpha)^{1+1/g}} \int_0^\infty \int_0^\infty d\tau_1 d\tau_2 e^{i\omega(\tau_1 + \tau_2)} \\ &\times \frac{(\tau_1 \tau_2)^{1/g}}{[(-\tau_1 - \tau_2 - t - i\alpha)(-\tau_1 - t - i\alpha)(-\tau_2 - t - i\alpha)]^{1/g}}, \end{aligned}$$

where we used the fact that the LL field operators satisfy the braiding relations, (19), with the braiding phase function

$$\varphi(t) = \frac{\pi}{g} \text{sign}(t). \quad (38)$$

Now we can perform the τ -integrations using the integral representation

$$\begin{aligned} (\tau_1 + \tau_2 - t - i\alpha)^{-1/g} &= \frac{e^{i\pi/2g}}{\Gamma(1/g)} \int_0^\infty dp p^{1/g-1} \\ &\times e^{-i(\tau_1 + \tau_2 - t)p}. \end{aligned}$$

Then

$$\begin{aligned} n_{>}(\omega) &= 2i\gamma^2 e^{-i\pi/g} \cos^2(\pi/2g) \quad (39) \\ &\times \int_{-\infty}^\infty dt \frac{e^{i(\omega-V)}}{(-t - i\alpha)^{1+1/g}} \\ &\times \Gamma^2(1/g + 1) \int_0^\infty dp p^{1/g-3} e^{ipt} \Psi^2(1/g, 0; -i(p + \omega)t), \end{aligned}$$

where Γ and Ψ are the gamma function and the Tricomi confluent hyper-geometric function, respectively [35]. Deforming the t -integration contour from the real axis to the contour around the branch cut of the function Ψ we arrive at a more convenient representation for the TED:

$$n_{>}(\omega) = A(g) \int_0^{V-\omega} dE \frac{E^{1/g-1}}{(E + \omega)^2} F_V(E + \omega), \quad (40)$$

where the spectral function is given by

$$\begin{aligned} F_V(p) &= 2 \text{Im} e^{-i\pi/g} \int_\alpha^\infty d\xi \xi^{-1/g-1} e^{-(V-p)\xi} \\ &\times \Psi^2(1/g, 0, -p\xi + i\alpha), \end{aligned} \quad (41)$$

and the pre-factor is

$$A(g) = \Gamma^2(1/g + 1) \gamma^2 \alpha^{2/g} \frac{\cos^2[\pi/2g]}{2\pi a_0^2 \Gamma(1/g)}.$$

In the limit of small energies, $\omega/V \ll 1$, the function Ψ is nearly constant and the limiting form of the spectral

function can easily be established:

$$F_V(p) \approx \frac{2\pi}{\Gamma^3(1+1/g)}(V-p)^{1/g}.$$

Therefore we obtain the following asymptotic form for the TED in vicinity of the Fermi edge

$$n(\omega) \approx C_2(\lambda+1)^2(\omega/V)^\lambda, \quad (42)$$

where $\lambda = 1/g - 2$ and C_2 is a numerical pre-factor regular at $\lambda = -1$.

We investigated the behaviour of the TED near the upper threshold $\omega = V$ by numerical evaluation of Eq. (40). The result is given by another power law:

$$n(\omega) \sim (V-\omega)^\nu, \quad \nu = \lambda + 2. \quad (43)$$

In the limit of weak interactions, $g \rightarrow 1$, the exponent λ approaches the perturbative result. Eq. (42) can be regarded as consisting of two factors. The first factor is the universal $1/\omega$ divergence inherent to all interacting 1D systems. The second factor reflects power-law renormalisations occurring in the LLs and, in particular, contains the local density of states (LDOS) of the primary electron. The latter object is suppressed for repulsive interactions ($g < 1$). So also the TED singularity is suppressed. At $g_c = 1/2$ the LDOS suppression effectively wins over and the singularity disappears. It is noteworthy that in the case when the interaction constant is smaller than this critical value, the TED has a maximum between the upper and lower thresholds $\omega = 0$ and $\omega = V$, as it is vanishing towards both limits.

In real systems the tunnelling amplitude γ is small. The secondary current is already calculated in the next-to-leading (compared to the primary current) approximation in γ . Still, it is a valid question to ask what happens at higher orders in the tunneling amplitude. For the case when the TED is divergent at the Fermi level ($\lambda < 0$), a small energy scale ω^* may emerge below which these higher order contributions become important. We do not currently have full answer to this question. Our preliminary calculations indicate, however, that the most divergent 4-th order diagram is the one for which Fig. 5 acts as self-energy. This would lead to the estimate $\omega^* \sim V\gamma^{-2/\lambda}$. This issue deserves further investigation.

Thus far we have discussed the spinless LL. The above results can be straightforwardly generalised to spinful systems such as quantum wires. Due to the spin-charge separation the LDOS at the end of the wire is then given by the same expression as in the spinless case with $1/g$ substituted by $(1/g_c + 1/g_s)/2$, where $g_{c,s}$ are the interaction constants in the charge and spin sectors, respectively [34]. Since the tunnelling processes conserve spin, the LDOS exponent is simply carried over to the TED, so that λ in Eq. (42) should be changed to:

$$\lambda \rightarrow \lambda = (1/g_c + 1/g_s)/2 - 2. \quad (44)$$

The relation between the lower and upper threshold exponents, Eq. (43), is still valid. When the spin SU(2) symmetry is preserved, it forces $g_s = 1$. The residual spin-backscattering interaction renormalises to zero under renormalisation group transformations (see [34] for a recent review on 1D physics and further references). However, the presence of an irrelevant operator should probably cause multiplicative logarithmic corrections to our power-law formula (42). We have not attempted to calculate these correction though we expect that this can be done by standard methods [36].

VI. TUNNELLING FROM 2D SYSTEMS: PURE LIMIT

In view of applications to MWNTs, we now consider tunnelling from a 2D electron system in tip geometry. Theoretically, this is a more complicated situation than in 1D. In some cases, relevant non-perturbative techniques exist, in other cases we shall present perturbative results. In this Section we discuss interacting 2D electron systems free from impurities (pure limit).

From the mathematical point of view we still have to calculate the same diagram [(a) in Fig. 4]. To accomplish this task in 2D it is convenient to change over to the momentum representation. The host Hamiltonian is $H[\psi] = H_0[\psi] + H_i[\psi]$, where

$$H_0[\psi] = \int \frac{d\vec{p}}{2\pi} \xi(\vec{p}) \psi_{\vec{p}}^\dagger \psi_{\vec{p}} \quad (45)$$

describes free 2D electron gas with dispersion relation $\xi(\vec{p})$ and $\psi_{\vec{p}}$ is the Fourier transform of the electron field operator. The interaction term has the standard form. In real space:

$$H_i = \int d\vec{r} d\vec{r}' \psi^\dagger(\vec{r}) \psi^\dagger(\vec{r}') U_0(|\vec{r} - \vec{r}'|) \psi(\vec{r}') \psi(\vec{r}), \quad (46)$$

where $U_0(r)$ is the interaction potential to be specified later. The relevant diagram is given by the following expression:

$$\begin{aligned} g_{>}^{-+}(\omega) &= \int \frac{d^2\vec{q}_1}{(2\pi)^2} \int \frac{d^2\vec{q}_2}{(2\pi)^2} \int \frac{d\Omega}{2\pi} \int \frac{d^2\vec{p}}{(2\pi)^2} \\ &\times g_0^{-}(\omega, \vec{p} - \vec{q}_1) g_0^{-+}(\omega - \Omega, \vec{p}) \\ &\times U_0(q_1) \Pi(\Omega; \vec{q}_1, \vec{q}_2) U_0(q_2) g_0^{-+}(\omega, \vec{p} - \vec{q}_2) \end{aligned} \quad (47)$$

Here $U_0(q)$ is the Fourier transform of the interaction potential, $\Pi(\Omega; \vec{q}_1, \vec{q}_2)$ stands for the inner polarisation bubble as in Fig. 4 (b) with vertex indices as in (a):

$$\begin{aligned} \Pi(\Omega; \vec{q}_1, \vec{q}_2) &= \int \frac{d\epsilon}{2\pi} \int \frac{d^2\vec{p}}{(2\pi)^2} g_0^{-}(\epsilon, \vec{p} + \vec{q}_1) \\ &\times G_0^{-+}(\epsilon) g_0^{-+}(\epsilon, \vec{p} + \vec{q}_2) g_0^{-+}(\epsilon + \Omega, \vec{p}). \end{aligned}$$

Without the tunnelling insertions, this would be a Keldysh analogy to the standard 2D Lindhard functions

[37]. We define $\vec{p} = P_\omega \vec{n}_\phi$ with a unit 2D vector \vec{n}_ϕ in direction parametrised by the angle ϕ . The quantity P_ω gives the on-shell magnitude of the momentum \vec{p} and, for a quadratic dispersion relation, satisfies the following equation,

$$\frac{P_\omega^2}{2m} = \frac{p_F^2}{2m} + \omega, \quad (48)$$

where p_F is the Fermi momentum and m is the effective

mass.

We change over from the momentum integration to the energy-angle integration in the standard manner:

$$\int \frac{d^2\vec{p}}{(2\pi)^2} \rightarrow \frac{1}{2\pi} \int d\xi \rho(\xi) \int_0^{2\pi} d\phi,$$

where $\rho(\xi)$ is the density of states in the host. The polarisation bubble can then be written in the form

$$\Pi(\Omega; \vec{q}_1, \vec{q}_2) = \rho_c \Theta(\Omega - V) \int_{-V}^{-\Omega} d\epsilon \rho(\epsilon + \Omega) \int_0^{2\pi} d\phi g_0^{--}(\epsilon, P_{\epsilon+\Omega} \vec{n}_\phi + \vec{q}_1) g_0^{++}(\epsilon, P_{\epsilon+\Omega} \vec{n}_\phi + \vec{q}_2),$$

where ρ_c stands for the constant density of states in the lead. The diagonal bare Keldysh Green's functions are

$$g_0^{--(++)}(\epsilon, P_{\epsilon+\Omega} \vec{n}_\phi + \vec{q}) = \mp \left[\Omega + \frac{1}{m} P_{\epsilon+\Omega} \vec{n}_\phi \vec{q} + \frac{1}{2m} q^2 \pm i0 \right]^{-1}.$$

In this expression we have taken into account the fact that $\epsilon < 0$ if we are only interested in $\omega > 0$ part of g^{-+} . The off-diagonal Keldysh function is

$$g_0^{-+}(\omega - \Omega, \vec{p}) = i2\pi n_F(\vec{p}) \delta(\omega - \Omega - \xi_{\vec{p}}),$$

where $n_F(\vec{p})$ is the Fermi momentum distribution function. Using these expressions and relation (8) between the Green's function and the TED we obtain a formula similar to Eq. (34) for the 1D case, namely

$$n_{>}(\omega) = \frac{\rho_c}{2\pi} \int_\omega^V d\Omega \rho(\omega - \Omega) \int_{-V}^{-\Omega} d\epsilon \rho(\epsilon + \Omega) \quad (49) \\ \times \int_0^{2\pi} d\phi d\phi' |F_\epsilon(\Omega, \phi - \phi')|^2,$$

where the function F is defined by

$$F_\epsilon(\Omega, \phi) = \frac{1}{4\pi^2} \int_0^\infty dq q U_0(q) \int_0^{2\pi} d\theta \\ \times \left[\Omega + \frac{1}{m} P_{\epsilon+\Omega} q \cos(\theta - \phi/2) + \frac{1}{2m} q^2 + i0 \right]^{-1} \\ \times \left[\Omega + \frac{1}{m} P_{\epsilon+\Omega} q \cos(\theta + \phi/2) - \frac{1}{2m} q^2 + i0 \right]^{-1}.$$

To proceed, we now need to specify the interaction potential. It is natural to start with a contact interaction term, $U(\vec{r} - \vec{r}') = U_0 \delta(\vec{r} - \vec{r}')$ or $U_0(q) = U_0$ in the momentum space. However, an unexpected technical difficulty arises. If we follow the standard practice and linearise the electron spectrum in the vicinity

of the Fermi surface, then the momentum integration in Eq. (50) can be easily done but the remaining angle integration diverges at $\varphi = \pm\pi$. This latter singularity comes from large momenta in the previous momentum integral and corresponds to the special case of hot hole back-scattering. To obtain a finite result for the TED one either needs to take into account the decay of $U_0(q)$ for large q or the non-linearity of the electron spectrum. Accordingly, we present two different calculations in the rest of this Section.

(i) Contact potential: $U_0(q) = U_0$.

First we scale the integration variable $q \rightarrow \Omega q$ and introduce dimensionless quantities $\gamma_{1,2} = P_{\epsilon\pm\Omega}/p_F$ and $\kappa = \Omega/4E_F$. Then,

$$F_\epsilon(\Omega, \phi) = \frac{U_0}{4\pi^2 v_F^2} \int_0^\infty dq q \int_0^{2\pi} d\theta \\ \times [1 + \gamma_1 q \cos(\theta - \phi/2) + \kappa q^2 + i0]^{-1} \\ \times [1 + \gamma_2 q \cos(\theta + \phi/2) - \kappa q^2 + i0]^{-1}.$$

Notice that γ 's approach unity whereas κ linearly tends to zero in the limit of small Ω . Furthermore, if we set $\kappa = 0$, the angle integration is still divergent. Therefore we set $\gamma_{1,2} = 1$ and keep κ finite. As a next step we expand the integrand in Eq. (50) using the standard formula [38],

$$\frac{1}{f(x) + i0} = \mathcal{P} \frac{1}{f(x)} - i\pi \delta(f(x)), \quad (50)$$

where \mathcal{P} denotes the principal value. This expansion produces three contributions: the first one contains the product of two principal parts and remains regular for $\Omega \rightarrow 0$, the second one contains products of one principal part and one delta function and is identically zero in the low energy regime, and the third contribution, F_ϵ^δ , containing a product of two delta functions is responsible for the divergency of the angle integral. Setting $v_F = 1$ for the rest of this Section, we write

$$F_\epsilon^\delta(\Omega, \phi) = \frac{U_0}{4\pi^2} \int_0^\infty dq q \int_0^{2\pi} d\theta \delta[1 + q \cos(\theta - \phi/2) + \kappa q^2] \delta[1 + q \cos(\theta + \phi/2) - \kappa q^2].$$

The evaluation of the angle integration leaves us with

$$F_\epsilon^\delta(\Omega, \phi) = \frac{U_0}{4\pi^2} \int_0^\infty dq q [q^2 - (1 + \kappa q^2)^2]^{-1/2} \delta[1 - (1 + \kappa q^2) \cos \phi + \sin \phi \sqrt{q^2 - (1 + \kappa q^2)^2 - \kappa q^2}].$$

The argument of the delta function is zero for

$$q_0^2 = \frac{1}{2\kappa^2} \sin^2(\phi/2) \left(1 - \sqrt{1 - 16 \frac{\kappa^2}{\sin^2 \phi}}\right).$$

Therefore the remaining momentum integration yields

$$F_\epsilon^\delta(\Omega, \phi) = \frac{U_0}{2\pi^2} \left[\sin \phi + \cos \phi \left(\sin \phi - \sqrt{\sin^2 \phi - 16\kappa^2} \right) - 4\kappa \sin \phi \right]^{-1}.$$

Plugging this expression into Eq. (49) and taking into account that for small Ω (and hence small κ) the main contribution to the angle integration originates for ϕ close to $\pm\pi$ one finds for the following limiting form for the TED:

$$n_{>}(\omega) \approx \frac{U_0^2}{8\pi^4} \rho_c \nu^2 E_F V \ln \left(\frac{V}{\omega} \right),$$

where $\nu = \rho(0)$.

(ii) Yukawa potential: $U_0(q) = 4\pi e^2 / \sqrt{q^2 + \lambda^2}$.

Here $1/\lambda$ is the screening length. As $U_0(q)$ now tends to zero for large q (which is, of course, always the case in real systems), we can linearise the dispersion relation. Then the function $F(\Omega, \phi)$ becomes independent of the energy variable ϵ and simplifies considerably:

$$F(\Omega, \phi) = \frac{1}{4\pi^2} \int_0^\infty dq q U_0(\Omega q) I(q, \phi), \quad (51)$$

where q has again been scaled by Ω and the function $I(q, \phi)$ is defined by

$$I(q, \phi) = \int_0^{2\pi} d\theta \left[(1 + q \cos(\theta - \phi/2) + i0) \times (1 + q \cos(\theta + \phi/2) + i0) \right]^{-1}. \quad (52)$$

This integral can be calculated and is real

$$I(q, \phi) = \frac{2\pi}{[1 - q^2 \cos^2(\phi/2)] \sqrt{1 - q^2}}, \quad (53)$$

for $q < 1$ but contains an imaginary part

$$I(q, \phi) = -i \frac{2\pi}{[1 - q^2 \cos^2(\phi/2)] \sqrt{q^2 - 1}} - \frac{\pi^2}{\sqrt{q^2 - 1} \cos(\phi/2)} \delta[q - 1/\cos(\phi/2)]. \quad (54)$$

for $q > 1$, as incoherent particle production takes place in the latter regime. Using Eqs. (53) and (54) we compute the momentum integral in Eq. (51) which yields

$$F(\Omega, \phi) = - \frac{2e^2}{|\sin(\phi/2)| \sqrt{\Omega^2 + \lambda^2 \cos^2(\phi/2)}} \times \operatorname{arccot} \left[\frac{\sqrt{\Omega^2 + \lambda^2 \cos^2(\phi/2)}}{\lambda |\sin(\phi/2)|} \right]. \quad (55)$$

Unfortunately we were not able to perform the last remaining angle integration in Eq. (49) in a closed form. However, to analyse the TED close to the Fermi surface $\omega \rightarrow 0$ one merely requires the knowledge of $|F(\Omega, \phi)|^2$ for small Ω 's. The latter can be easily read off Eq. (55) for $\Omega \ll \lambda$. There are two different regions in the parameter space (ϕ, Ω) : for most angles, $|\phi \pm \pi| > 2\Omega/\lambda$, we find

$$|F(\Omega, \phi)|^2 \approx \frac{4e^4}{\lambda^2} \frac{\phi^2}{\sin^2 \phi}$$

whereas for large scattering angles $|\phi \pm \pi| < 2\Omega/\lambda$ one obtains a singular in Ω behaviour,

$$|F(\Omega, \phi)|^2 \approx \frac{\pi^2 e^2}{\Omega^2}.$$

The latter region, physically corresponding to hot hole back-scattering processes, is responsible for the leading contribution to the remaining integrals. With logarithmic accuracy we thus obtain the following threshold behaviour of the TED,

$$n_{>}(\omega) \approx \rho_c \nu^2 \frac{2\pi e^4}{\lambda} \ln \left[\frac{\max(V, \lambda)}{\omega} \right]. \quad (56)$$

Clearly the same logarithmic singularity will persist for other functional forms of $U_0(q)$ as long as it decays for large q . (We note that in the purely Coulomb case, $\lambda = 0$, an additional divergence at small q is introduced. Calculation shows that all the divergences cancel exactly in this special case with the second order result for the TED being identically zero for all $\omega > 0$. The physical meaning of this observation escapes us.)

The net result is that we find a logarithmic singularity in the TED for 2D electron systems at the second order in the interaction. Such behaviour is in apparent contradiction with Ref. [7] where a stronger singularity

was found. These differences may be due to the fact that Gadzuk and Plummer analysed a different set-up with a three-dimensional host and a 2D emitting surface (as opposed to our set-up with a 2D host and tip emission), or their stronger singularity may be an artifact of the low-density approximation. This issue as well as the role of higher-order scattering processes deserve more intensive study and will be discussed elsewhere. In view of applications to MWNTs, however, there are two more immediate questions: the role of the dynamical Coulomb screening and of the disorder potential. Both require a non-perturbative approach and will be discussed in the next Section.

VII. TUNNELLING FROM DISORDERED 2D SYSTEMS

Contrary to the SWNTs, MWNTs can be described by the LL theory only in some special cases when the radii of outer shells are not too large [39]. Otherwise their physics is best described in terms of a disordered 2D electron liquid with Coulomb interaction. Such systems have been extensively studied in the 80's using non-linear sigma model and renormalisation group [40, 41, 42]. Recently they attracted more attention due to the discovery of a possible metal-insulator transition in MOSFETs [43], which stimulated further theoretical research. Kamenev and Andreev (KA) [44] have recently examined the Keldysh non-linear sigma model [45] for the Coulomb case (long-range interaction). In this Section we apply their method to obtain the threshold behaviour of the TED for tunnelling from a 2D interacting disordered metal.

The Hamiltonian of the previous Section, composed from (45) and (46) with $U_0(q) = 4\pi e^2/q$, should now be supplemented by the disorder term

$$H_d[\psi] = \int d\vec{r} V(\vec{r}) \psi^\dagger(\vec{r}) \psi(\vec{r}) \quad (57)$$

with a δ -correlated Gaussian disorder potential $V(\vec{r})$.

The formal procedure of deriving the Keldysh sigma model is described in the relevant literature ([44, 45], see also [46]) in detail. Therefore we only give a brief outline here. One starts with the Keldysh S -matrix. (This object is identically unity but it becomes a generating functional upon introducing auxiliary fields. If one wants to start with a diagonal bare Keldysh function, the contour is different from that in Fig. 2, see explanation in Refs. [45, 46]). One can then integrate the disorder out obtaining a non-local in time four-fermion interaction term. The action is made quadratic in fermions by applying the Hubbard-Stratonovich transformation to the latter term as well as to the Coulomb interaction term. Hence there are two decoupling fields, Q and Φ in the notation of Ref. [44]. The fermions can now be formally integrated out resulting in the following expression for the generat-

ing functional [44]:

$$\langle Z \rangle = \int \mathcal{D}\Phi e^{i\text{Tr}(\Phi^T U_0^{-1} \sigma_1 \Phi)} \int \mathcal{D}Q e^{iS[Q, \Phi]}. \quad (58)$$

with the sigma-model action (after Keldysh rotation)

$$iS[Q, \Phi] = -\frac{\pi\nu}{4\tau} \text{Tr} Q^2 + \text{Tr} \ln[G_0^{-1} + \frac{i}{2\tau_0} Q + \phi_\alpha \gamma^\alpha + \zeta],$$

Here τ_0 is the elastic mean free time and U_0 stands for the unscreened interaction potential. The decoupling field Q depends on two time variables and is a 2×2 matrix in the Keldysh space. The decoupling field Φ is a Keldysh doublet $(\phi_1, \phi_2)^T$. The vertex matrices are defined as follows:

$$\gamma^1 = \begin{pmatrix} 1 & 0 \\ 0 & 1 \end{pmatrix}, \quad \gamma^2 = \sigma_1 = \begin{pmatrix} 0 & 1 \\ 1 & 0 \end{pmatrix}.$$

Doing the functional variation of the generating functional, (58), with respect to the auxiliary field ζ and setting the latter to zero one obtains the complete set of single-particle Green's functions:

$$\frac{\delta}{\delta\zeta} \langle Z \rangle \Big|_{\zeta=0} = \begin{pmatrix} G^R & G^K \\ 0 & G^A \end{pmatrix} = \mathcal{G}.$$

where the function $G^K = (G^R - G^A)(1 - 2n(E))$ is related to the single-particle energy distribution function $n(E)$ and $G^{R(A)}$ are the retarded and advanced Green's functions, respectively.

We need to calculate of the four-point correlation function $\mathcal{K}_{+-}^+(t_2, t_3; t_1, t_4)$. (A calculation of a different four-point function for a non-equilibrium noise problem has recently been done within a similar framework in [47].) This can be achieved by double variation of the generating functional with respect to the auxiliary field ζ :

$$\mathcal{K}_{+-}^+(t_2, t_3; t_1, t_4) = \int \mathcal{D}\Phi e^{i\text{Tr}(\Phi^T V_0^{-1} \sigma_1 \Phi)} \int \mathcal{D}Q e^{iS[Q, \Phi]} \times [W(t_1, t_4) \otimes W(t_3, t_2) + W(t_1, t_2) \otimes W(t_3, t_4)]_* \quad (59)$$

where

$$W(t_1, t_2) = \left[G_0^{-1} + \frac{i}{2\tau_0} Q + \phi_\alpha \gamma^\alpha \right]^{-1}.$$

A functional integral of this type with a single W function yields the Green's function matrix \mathcal{G} and was discussed in [44]. A product of two and more W functions produces a complicated object, which is a tensor product containing all possible time orderings. The operation of extracting the particular component corresponding to \mathcal{K}_{+-}^+ we denote by $[\dots]_*$. At this stage its exact definition is unimportant and we postpone it to the end of the Section.

We now evaluate the functional integral with the product of two W -functions in the saddle point approximation following KA's approach [44]. In this case

$$W(t, t') = -i\pi\nu e^{ik_\alpha(t)\gamma^\alpha} \Lambda(t-t') e^{ik_\alpha(t')\gamma^\alpha}, \quad (60)$$

where $\Lambda(t)$ denotes the mean-field non-interacting Green's function matrix in equilibrium (corresponding to non-crossing disorder diagrams [26]) and $k_\alpha(t)$ is a linear functional of Φ . The corresponding correlation matrix with respect to averaging over the ϕ -fields is given by [44]:

$$\langle k_\alpha(q, \omega) k_\beta(-q, -\omega) \rangle_\Phi = \frac{i}{2} \mathcal{V}_{\alpha\beta}(q, \omega), \quad (61)$$

$$\begin{aligned} \mathcal{V}_{\alpha\beta}(q, \omega) &= \begin{pmatrix} \mathcal{V}^R(q, \omega) & \mathcal{V}^R(q, \omega) \\ \mathcal{V}^A(q, \omega) & 0 \end{pmatrix} \\ \mathcal{V}^{R(A)}(q, \omega) &= -\frac{1}{(dq^2 \mp i\omega)^2} \left[\frac{1}{V_0} + \frac{\nu dq^2}{dq^2 \mp i\omega} \right]^{-1} \\ \mathcal{V}^K &= n_B(\omega) (\mathcal{V}^R(q, \omega) - \mathcal{V}^A(q, \omega)), \end{aligned} \quad (62)$$

where $n_B(\omega)$ is the Bose distribution function and d is the electron diffusion constant. Using the saddle point representation in Eq. (60) the product of two W -functions can be re-written as

$$\begin{aligned} &\langle [W(t_1, t_4) \otimes W(t_3, t_2)]_* \rangle_\Phi \\ &= \frac{1}{4} \sum_{\mu_i} [(\gamma^{\mu_1} \Lambda(t_1, t_4) \gamma^{\mu_4}) \otimes (\gamma^{\mu_3} \Lambda(t_3, t_2) \gamma^{\mu_2})]_* \\ &\times \langle p_{\mu_1}(t_1) (p_{\mu_4}(t_4))^* p_{\mu_3}(t_3) (p_{\mu_2}(t_2))^* \rangle_\Phi. \end{aligned} \quad (63)$$

The operation of taking the correct time ordering is now separated from of the averaging over the field Φ , which only affects the objects

$$\begin{aligned} p_\mu(t) &= e^{i(k_1(t)+k_2(t))} + \mu e^{i(k_1(t)-k_2(t))} \\ = s(t) + \mu \bar{s}(t) &= e^{i\alpha(k_1(t)+\beta k_2(t))} + \mu e^{i\alpha(k_1(t)-\beta k_2(t))}. \end{aligned}$$

The product of four p_μ -operators is a sum of 16 products of different $s(t_i)$ -operators. The latter objects can be evaluated using the correlation matrix, Eq. (61),

$$\begin{aligned} &\langle e^{i\alpha_1(k_1(t_1)+\beta_1 k_2(t_1))} e^{-i\alpha_4(k_1(t_4)+\beta_4 k_2(t_4))} \\ &\times e^{i\alpha_3(k_1(t_3)+\beta_3 k_2(t_3))} e^{-i\alpha_2(k_1(t_2)+\beta_2 k_2(t_2))} \rangle_\Phi \end{aligned}$$

$$\begin{aligned} &= \exp \left\{ -\frac{i}{2} \left[\alpha_1 \alpha_3 \mathcal{V}_{13}(\beta_1, \beta_3) - \alpha_1 \alpha_4 \mathcal{V}_{14}(\beta_1, \beta_4) \right. \right. \\ &- \alpha_4 \alpha_3 \mathcal{V}_{43}(\beta_4, \beta_3) + \alpha_4 \alpha_2 \mathcal{V}_{42}(\beta_4, \beta_2) \\ &\left. \left. - \alpha_3 \alpha_2 \mathcal{V}_{32}(\beta_3, \beta_2) - \alpha_1 \alpha_2 \mathcal{V}_{12}(\beta_1, \beta_2) + 2\mathcal{V}_0(\beta_1, \beta_1) \right] \right\}, \end{aligned} \quad (64)$$

where we use the following definition

$$\begin{aligned} \mathcal{V}_{ij}(\beta_i, \beta_j) &= \mathcal{V}^K(t_i - t_j) + \beta_i \mathcal{V}^A(t_i - t_j) \\ &\quad + \beta_j \mathcal{V}^R(t_i - t_j). \end{aligned} \quad (65)$$

Taken separately these functions are divergent. Nevertheless Eq. (64), being rewritten as a function of differences $\mathcal{V}_{ij}(\beta_i, \beta_j) - \mathcal{V}_{ii}(\beta_i, \beta_i)$, can be made convergent. In this case a special selection rule has to be fulfilled,

$$\begin{aligned} &\alpha_1 \alpha_3 \mathcal{V}_0(\beta_1, \beta_3) - \alpha_1 \alpha_4 \mathcal{V}_0(\beta_1, \beta_4) \\ &- \alpha_4 \alpha_3 \mathcal{V}_0(\beta_4, \beta_3) + \alpha_4 \alpha_2 \mathcal{V}_0(\beta_4, \beta_2) \\ &- \alpha_3 \alpha_2 \mathcal{V}_0(\beta_3, \beta_2) - \alpha_1 \alpha_2 \mathcal{V}_0(\beta_1, \beta_2) \\ &+ \frac{1}{2} \sum_{j=1, \dots, 4} \mathcal{V}_0(\beta_j, \beta_j) = 0, \end{aligned} \quad (66)$$

otherwise (64) is divergent. Using Eqs. (62) one can calculate the asymptotic behaviour of $\mathcal{V}_{ij}(\beta_i, \beta_j) - \mathcal{V}_{ii}(\beta_i, \beta_i)$ for large time differences (to calculate the limiting Fermi edge asymptotics of the TED this knowledge is sufficient as we shall see shortly). Fortunately, the limiting form turns out to be independent of the arrangement of the β -indices, with the result

$$\mathcal{V}_{ij}(\beta_i, \beta_j) - \mathcal{V}_{ii}(\beta_i, \beta_i) \approx i \frac{e^2}{4\pi f} \ln^2 \left| \frac{f^2(t_i - t_j)}{d} \right|,$$

where $f = 2\pi e^2 \nu d$. The last average in Eq. (63) is then given by

$$\begin{aligned} &\langle p_{\mu_1}(t_1) (p_{\mu_4}(t_4))^* p_{\mu_3}(t_3) (p_{\mu_2}(t_2))^* \rangle_\Phi \\ &= \left(\prod_j (1 + \mu_j) \right) \langle s(t_1) s^*(t_4) s(t_3) s^*(t_2) \rangle_\Phi. \end{aligned}$$

Obviously, the above is nonzero only if for all i $\mu_i = +1$. That means that we can set all α_j 's equal as well. Such choice automatically fulfils the selection rule, (66). Therefore the full four-point correlation function is given by

$$\mathcal{K}_{+-}^-(t_1, t_2; t_3, t_4) \approx Y(t_1, t_2; t_3, t_4) \exp \left(-\frac{e^2}{8\pi f} \left\{ \ln^2 \left| \frac{f^4(t_1 - t_4)(t_4 - t_3)(t_3 - t_2)(t_1 - t_2)}{d^2(t_1 - t_3)(t_4 - t_2)} \right| \right\} \right) \quad (67)$$

with

$$Y(t_1, t_2; t_3, t_4) = [(\gamma^1 \Lambda(t_1, t_4) \gamma^1) \otimes (\gamma^1 \Lambda(t_3, t_2) \gamma^1)]_*.$$

The latter expression is basically the non-interacting four-point correlation function with special time order-

ing and is equal to $G^{+-}(t_1 - t_4)G^{+-}(t_3 - t_2)$. The second term in Eq. (59) can be calculated in a similar manner resulting in the same, up to an interchange of time variables, exponential factor as in Eq. (67) and an appropriate pre-factor. The pre-factors can in principle be re-exponentiated but this would only result in logarithmic corrections which can be neglected in comparison to the main disorder part. In order to use formula (15), we substitute $t_1 = \tau_1$, $t_3 = 0$, $t_2 = t + \tau_1$ and $t_4 = t + \tau_1 + \tau_2$. We are interested in the low-energy regime $\omega/V \ll 1$. Therefore the lower limit for the time integrations can be set to $1/D$ (D being the conductance band-width) if it causes divergences and to zero otherwise. Thus we obtain

$$n_{>}(\omega) \sim \int_0^\infty d\tau_1 \int_0^\infty d\tau_2 e^{i\omega(\tau_1 + \tau_2)} \times \exp \left\{ -\frac{e^2}{8\pi f} \ln^2 \left| \frac{f^4(\tau_1 + \tau_2)}{d^2 D} \right| \right\}.$$

Estimating the τ -integrals for small ω yields the final result for the TED in vicinity of the Fermi edge:

$$n_{>}(\omega) \sim \exp \left[-\frac{e^2}{8\pi f} \ln^2 \left(\frac{d^2 D}{f^4 \omega} \right) \right]. \quad (68)$$

Thus we find that the combined effect of the disorder and the Coulomb interaction is to suppress the TED towards the Fermi surface. This result can be understood in terms of the well known Altshuler-Aronov-Lee anomaly [48] in the density of states of the primary electrons. Indeed, one of the important results of the KA's work [44] was to show that the negative logarithmic correction to the density of states can be exponentiated (and becomes a double-log due to the long-range Coulomb forces). Our formula (68) achieves a similar exponentiation for the TED. As in [44], this is only valid above certain energy scale ϵ^* , due to the on-set of the fluctuation effects (corrections to the saddle-point approximation). In MWNTs the situation is further complicated by the dimensional cross-over effect; the corresponding energy scale $\epsilon^* \simeq d/L^2$ (L being the tube's circumference) was estimated in [20], see also [49] for further discussion.

VIII. FIELD EMISSION FROM CARBON NANOTUBES

Field emission setup is relatively simple. An electric field of strength F is applied between a metallic tip of the emitter and a counter-electrode which are usually placed in a vacuum. Superposition of the confinement potential, the image potential and the electrostatic potential due to the external electric field leads to a formation of a barrier with a finite width allowing the electrons to tunnel out of the emitter even at zero temperatures, Fig. 6. Therefore the FE process can be regarded as tunnelling into vacuum through a triangularly-shaped barrier whose upper part is rounded off by the image potential. However, at low

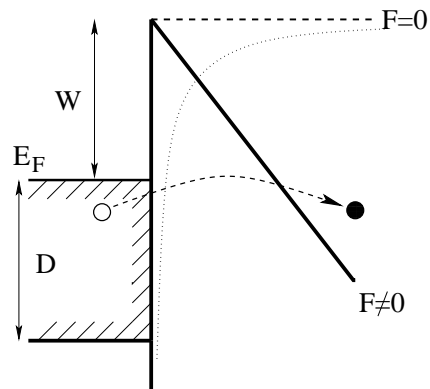


FIG. 6: Schematic representation of the field emission setup. Here F is the applied electric field, W is the work function and D is the conduction band-width. The dashed line represents the confining potential without field and the dotted line stands for the image potential.

temperatures the larger part of tunnelling electrons will have energies close to the Fermi energy, so the exact form of the barrier is unimportant.

Quantities of interest are the energy-resolved current $j(\omega)$ and the total current J . If the tunnelling amplitude is small (which it is for all real systems), then $j(\omega)$ is proportional to the probability $n(\omega)$ for an electron to have energy ω , to the energy dependent transmission coefficient $\mathcal{D}(\omega)$, and to a factor \mathcal{F} responsible for the tip geometry:

$$j(\omega) = \mathcal{F}\mathcal{D}(\omega)n(\omega). \quad (69)$$

In the noninteracting case and neglecting higher-order tunnelling processes, $n(\omega)$ coincides with the Fermi distribution function multiplied by the LDOS. The (quasi-classical) transmission probability for a triangular barrier is given by [50]:

$$\mathcal{D}(\omega) \sim \exp(-4\sqrt{2m}(W - \omega)^{3/2}/3\hbar F), \quad (70)$$

where m is the electron mass and W is the work function. As discussed e. g. in Ref. [2], the transmission coefficient is only slightly affected by the image potential and for the field strength $F \ll (W - E_F)^2/e^3$ the barrier can be regarded as strictly triangular. At zero temperatures, the emerging (primary) spectrum has a sharp threshold at the Fermi energy (no particles above E_F) and is essentially constant in its vicinity.

The general picture does not change much even in the case of interacting electrons. For the LLs $n(\omega)$ is proportional to the relevant LDOS, which is known [28, 34] to be

$$n(\omega) = \Theta(-\omega)|\omega|^{1/g-1}/a_0 D^{1/g} \Gamma(1/g). \quad (71)$$

Plugging this into Eq. (69) one observes that at this lowest order in the tunnelling the TED above the Fermi energy is still zero, even for the strongly correlated LL.

Below the Fermi energy the TED has a power-law singularity. Expanding the transmission coefficient in powers of ω/W (work function being the largest energy scale), and integrating over all energies we establish the Fowler-Nordheim (FN) formula for LLs:

$$J = \frac{\mathcal{F}}{a_0 D^{1/g}} \left[\frac{F^2}{4k_F W} \right]^{1/2g} \exp \left(-\frac{4k_F^{1/2}}{3F} W^{3/2} \right), \quad (72)$$

relating the full current to the electric field's strength [2, 8].

The generalisation of these results for SWNTs is rather straightforward. Indeed, these systems are known to be described as four-channel LLs. Three channels ϕ_{c-} (charge-flavour), ϕ_{s+} (total spin), ϕ_{s-} (spin-flavour) are non-interacting. The fourth channel ϕ_{c+} (total charge, or the plasmon mode) possesses the LL parameter $K = (1 + 4U_0/\pi)^{-1/2}$, where U_0 is the zero Fourier component of the screened Coulomb potential. Note that though we now have four channels the field-operator actually factorises as [12, 13, 14]

$$\psi \sim \exp\{i\phi_{c+}/(2\sqrt{K}) + i(\phi_{c-} + \phi_{s+} + \phi_{s-})/2\}. \quad (73)$$

Just as in the case of the spinless LL, the interaction constant K is included into the rescaled Bose fields and disappears from the Hamiltonian, which is given by

$$H = \frac{1}{4\pi} \sum_{\delta=c,s,j=\pm} \int dx (\partial_x \phi_{\delta j})^2. \quad (74)$$

All the correlation functions also factorise. Hence the results for the LDOS [28, 34] as well as the results of Section V, Eqs. (42) and (43), are still valid for SWNTs given that the substitution

$$g^{-1} \rightarrow (K^{-1} + 3)/4. \quad (75)$$

is made.

The typical value for K in SWNTs lies near 0.2 (0.15 to 0.3), which fixes the effective g to ≈ 0.5 [12, 13, 14, 15, 16]. As a result, Eq. (72) is reasonably well approximated by the classical FN law. This fact offers one possible explanation as to why the experimental data of Refs. [24, 51] can be relatively well fitted by the conventional FN curve. In addition, all the experiments currently available were made on SWNT films where the nanotubes build a network with essentially a random 2D geometry. This case, when extra complications are bound to arise, is beyond the scope of this paper. To straightforwardly reveal the correlation effects in the primary current, measurement on a *single* SWNT are more appropriate. To our knowledge, this has not been done yet.

Let us now discuss the secondary current. The analysis of the secondary effects can also be made in terms of tunnelling into vacuum. Thereby we should bear in mind that the theory presented in Section III assumes that

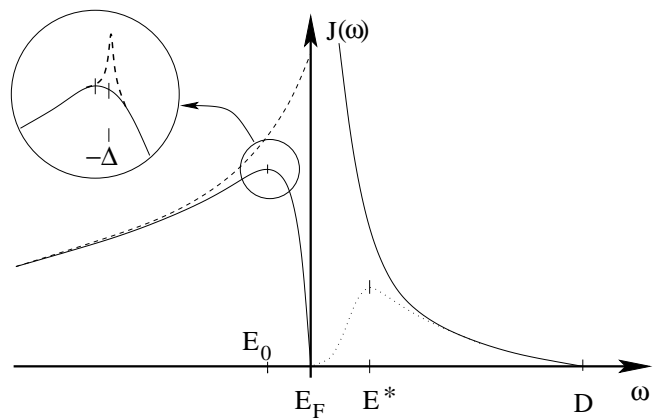


FIG. 7: A sketch of the energy resolved current in a field emission process from LLs. An additional Lorentz peak due to tunnelling through a localised level (if exists) is depicted in the inset.

the tunnelling amplitude is energy independent. Therefore, since the effective applied voltage is large in the FE setup (one has to send the chemical potential on the right electrode to minus infinity), some integrals inevitably diverge. To overcome this difficulty and to make the theory more quantitative, we now recall that there are two candidates that can be used as the effective voltage. The first one is the characteristic energy scale in the exponential transmission coefficient $\mathcal{A} = F/2(k_F W)^{1/2}$, see Eq. (70). The second one is the width of the emitter conductance band D . Therefore the high-energy cutoff playing the role of V in the FE setup is either D or \mathcal{A} , whichever is smaller. We shall use D through the rest of the paper. With this modification all results of the previous Sections for the TED $n(\omega)$ are valid with the understanding that the tunnelling probability is proportional to the transmission coefficient of the barrier at the Fermi energy, $\gamma^2 \sim \mathcal{D}(E_F)$. According to Eqs. (7) and (8) the secondary current is proportional to the TED. For SWNT the TED possesses all the singularities characteristic for LLs, which we have already discussed. One thing worth noting is that the critical value of the coupling now is $K_c = 1/5$, which is actually within the experimental range. Therefore we do not make a specific prediction regarding the character of the singularity (divergent versus convergent TED at the Fermi edge). Instead we think that both the divergent and the vanishing TEDs can be observed depending on the experimental setup. Unfortunately, in most recent experiments, both on SWNTs and MWNTs, only the total current is measured. Where the energy-resolved measurements were actually made [24, 51, 52], in all cases but one, the temperatures were too high for the secondary effects to be visible. To our knowledge, so far only the experiments of Ref. [27] contain high-energy tails which can be attributed to secondary emission. However, the quality of the presented data hinders us from attempting to actually fit the curves.

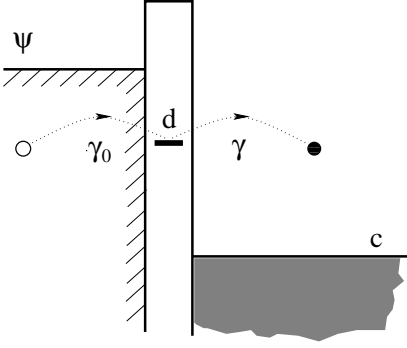


FIG. 8: A schematic representation of the electron tunnelling through a localised state d .

We conclude this Section by summarising our scenario for the energy resolved current in the FE from LLs (and SWNTs). Well below the Fermi energy $j(\omega)$ is governed by the exponential growth of the transmission coefficient, $j(\omega) \sim \exp(\omega/\mathcal{A})$, see Fig. 7, as is the case for any metallic emitter. Nearing the Fermi level, at energies given by $E_0 \approx (1 - 1/g)\mathcal{A}$, the non-linear LL LDOS effects win over the exponential growth resulting in a maximum in the current profile $j(\omega)$. Further towards the Fermi energy it decreases according to the power-law: $\sim |\omega|^{1/g-1}$. The edge behaviour right above E_F is given by $\sim \omega^{1/g-2}$. This changes shape depending on whether g is smaller or larger than the critical coupling g_c . In the case of weak interactions, $1/2 < g < 1$, there is a singularity, while for strong correlations, $0 < g < 1/2$ this singular behaviour is suppressed and there is a power-law approach to zero. In the latter case $j(\omega)$ acquires an additional maximum at a cross-over energy E^* . For small applied fields, there is an upper threshold at energy $\min(D, \mathcal{A})$ where the energy resolved current behaves as $\sim (\min(D, \mathcal{A}) - \omega)^{1/g}$.

IX. TUNNELLING VIA LOCALISED STATES

Recent luminescence spectra measurements in FE experiments on carbon nanotubes [24, 27] suggest that, at least in some cases, the emission process cannot be understood simply in terms of tunnelling into vacuum. They rather seem to be compatible with a model where the emitted electron tunnels out of the system through one or more localised states at the tip of the emitter [24, 27]. In this Section, we generalise our formalism in order to analyse such a multiple stage tunnelling.

We start with the Hamiltonian of the system. Contrary to Eq. (1), the transfer of an electron between the host and the lead occurs in two stages. At the first stage, the electron populates a localised level with energy $-\Delta$, see Fig. 8. Let the tunnelling amplitude for this process be γ_0 . At the second stage the electron tunnels from the localised state into the lead,

$$H_2 = H[\psi] + H_0[c] + \gamma_0 [\psi(0)^\dagger d + d^\dagger \psi(0)] + \gamma [d^\dagger c(0) + c^\dagger(0)d] - \Delta d^\dagger d, \quad (76)$$

where we retain the notation γ for the tunnelling amplitude of the second process and d^\dagger, d are the creation and annihilation operators of the localised state, respectively. We assume that $0 < -\Delta < -V$. This is not restrictive but reasonable. Indeed, the first inequality reflects the fact that the electric field applied to the emitter causes an effective lowering of energy of the states close to the tip. The second inequality is a trivial one because if the energy of the state d lied below both Fermi levels it would have always been populated. For simplicity, we neglect any electrostatic interaction between the localised state and the leads and the Hubbard term for d . Like in the case of the simple tunnelling, the lead is assumed to be uncorrelated.

The problem of a localised state hybridised with a non-interacting continuum is, of course, exactly solvable [1]. Therefore one way to proceed would be to eliminate the γ hopping term from the Hamiltonian exactly and then apply perturbation theory in γ_0 . However, in the FE setup Δ is expected to be much smaller than the conductance band width D . This implies that $\gamma_0 \gg \gamma$. Therefore we take an alternative route and first calculate the TED of the electrons on the level d as a function of $g^{-+}(\omega)$ in the host ignoring tunnelling to the lead. (We did the alternative calculation as well and, at a given order of perturbation theory, obtained exactly the same results.) To proceed we define the Keldysh Green's function of the localised level:

$$D(t) = -i \langle T_C [d(t) d^\dagger(0) S_C] \rangle, \quad (77)$$

where the S -matrix includes only the tunnelling between the host and the localised level,

$$S_C = T_C \exp \left(-i \gamma_0 \int_C dt [\psi^\dagger(0, t) d(t) + d^\dagger(t) \psi(0, t)] \right).$$

Expanding the Green's function (77) and function $\langle T_C [d(t) \psi^\dagger(0, t') S_C] \rangle$ in powers of γ_0 one obtains a set of coupled equations for them. Eliminating the latter object one then obtains the following Dyson-type equation for the Keldysh Green's function:

$$D(t, t') = D_0(t, t') + \int_C dt'' D(t, t'') \kappa(t'', t'), \quad (78)$$

where the kernel is given by

$$\kappa(t'', t') = \gamma_0^2 \int_C dt g_0(t'', t) D_0(t, t'). \quad (79)$$

Here $g_0(t, t')$ and $D_0(t, t')$ denote the Green's functions of the host and the localised level in the absence the hopping term. Disentangling the Keldysh indices and Fourier transforming we obtain the following set of equations:

$$D^{-+}(\omega) = D_0^{-+}(\omega) + D^{-+}(\omega) \kappa^{-+}(\omega) - D^{-+}(\omega) \kappa^{++}(\omega), \\ D^{--}(\omega) = D_0^{--}(\omega) + D^{--}(\omega) \kappa^{--}(\omega) - D^{-+}(\omega) \kappa^{+-}(\omega).$$

The solution is given by

$$D^{-+}(\omega) = \frac{D_0^{-+} + \gamma_0^2 g_0^{-+}(\omega) |D_0^{--}(\omega)|^2}{1 + 2\gamma_0^2 \text{Re}[g_0^{--}(\omega) D_0^{--}(\omega)] + \gamma_0^4 |g_0^{--}(\omega) D_0^{--}(\omega)|^2}. \quad (80)$$

This equation can be further simplified if one takes into account that $\text{Re}[g_0^{--}(\omega)]/|D_0^{--}(\omega)|^2$ vanishes for our system. Then the TED on the localised level is proportional to

$$D^{-+}(\omega) = \frac{\gamma_0^2 g^{-+}(\omega)}{(\omega + \Delta)^2 + \gamma_0^4 |g^{--}(\omega)|^2}. \quad (81)$$

In the last relation we omitted the subscript 0 of $g(\omega)$ functions. Strictly speaking this constitutes an approximation. The reason is that since the tunnelling onto the localised level affects the Green's function of the host they have to be calculated self-consistently. However, the renormalisations occurring close to the Fermi energy should not strongly affect the shape of the localised state and vice versa. That is unless the localised level becomes resonant ($\Delta \rightarrow 0$), which case we shall not consider in this paper. (We note though that the resonant level case can be approached via a mapping onto the Kondo problem [53].) For a non-interacting host $|g^{--}(\omega)|^2$ is simply a constant equal to $1/4v_F^2$.

As we know from Section III, the TED in the non-interacting lead, is proportional to $D^{-+}(\omega)$ and the tunnelling probability γ^2 :

$$n(\omega) = -i\gamma^2 D^{-+}(\omega). \quad (82)$$

We now briefly discuss the picture for a non-interacting emitter. According to Eq. (81) there is a Lorentzian peak at $\omega = -\Delta$ with height $4v_F^2 g^{-+}(-\Delta)/\gamma_0^2$ and width $\gamma_0^2/2v_F$. At the second order in γ^2 , there still is a sharp threshold at the Fermi energy. These results for non-interacting emitters are, of course, known (see e. g. [2]). Here we have merely re-derived them using the Keldysh formalism.

Let us now turn to the open question of how the presence of a localised state would modify the FE process from a LL. For the primary current we can still use formula (69), where we have to substitute the TED of the electrons in the host by that of the electrons on the localised state. The energy resolved current is then given by the following expression (we again set $v_F = 1$),

$$\begin{aligned} \mathcal{J}(\omega) &= -i\mathcal{F}\mathcal{D}(\omega) D^{-+}(\omega) \\ &= \frac{\mathcal{F}\gamma^2\gamma_0^2 \Theta(-\omega)}{a_0 D^{1/g} \Gamma[1/g]} \frac{|\omega|^{1/g-1}}{(\omega + \Delta)^2 + \gamma_0^4/4} \\ &\times \exp\left(-4k_F^{1/2} \frac{(W - \omega)^{3/2}}{3F}\right). \end{aligned} \quad (83)$$

In comparison to the situation without the localised level, there is an additional feature: the Lorentzian resonance at $\omega = -\Delta$. To compute the total emitted current we

re-write the energy integral in terms of the dimensionless variable $\xi = \omega/\mathcal{A}$ and expand the exponent in powers of ω/W as the work function is large compared to other energy scales. The total current then is

$$\begin{aligned} \mathcal{J} &= \frac{\gamma^2\gamma_0^2 \mathcal{F}}{a_0 D^{1/g} \Gamma[1/g]} \exp\left(-4k_F^{1/2} \frac{W^{3/2}}{3F}\right) \mathcal{A}^{1/g-2} \\ &\times \int_0^\infty d\xi \frac{\xi^{1/g-1}}{(\xi - \Delta/\mathcal{A})^2 + (\gamma_0^2/2\mathcal{A})^2} e^{-\xi}. \end{aligned} \quad (84)$$

This integral can be calculated exactly, resulting in the modified FN relation

$$\mathcal{J} = J \frac{2\gamma_0^2}{\mathcal{A}} \text{Im} \left\{ w^{1/g-1} e^w \Gamma[1 - 1/g, w] \right\}$$

applicable for arbitrary parameters. Here J is the total current in the absence of the localised state, see Eq. (72), Γ stands for the (incomplete) gamma function and we have introduced a dimensionless quantity w , defined by

$$w = \frac{1}{\mathcal{A}} (i\gamma_0^2/2 - \Delta).$$

There two important limiting cases.

(i) The electric field is weak, $\Delta/\mathcal{A} \gg 1$, or $\Delta \gg F/2(k_F W)^{1/2}$. Then the resonance peak is far away from the Fermi edge in comparison with the characteristic decay scale of the transmission coefficient. The result of the integration in Eq. (84) is then essentially identical to the result for a system without a localised level Eq. (72), up to numerical pre-factors. Therefore we would not expect that in this regime one can differentiate between the direct tunnelling and tunnelling via a localised state.

(ii) The electric field is sufficiently strong, so that $\Delta/\mathcal{A} \ll 1$. Now the distance from the resonance to the Fermi edge is much smaller than the characteristic energy scale \mathcal{A} . If also $\gamma^2 \ll \Delta$ (which is to be expected) the total current is still given by Eq. (72), apart from the overall pre-factor, but with a different exponent: $1/2g$ should now be substituted by $1/2g - 1$. This change can be important for the analysis of experimental data on the SWNTs. For SWNTs in this regime, we expect the modified FN plot to be linear in the coordinates $\ln[\mathcal{J}/F^{(1/K-5)/4}]$ and $1/F$. For $K \approx 0.2$ the total current depends exponentially on the field strength (not a stretched exponential).

The calculation of the secondary current is more delicate. In the case of the localised state the insertion in the diagram for $g^{-+}(\omega)$, see Figs. 4 and 5, should be modified. It turns out that there is only one way to dress the Green's function G_0^{+-} with the Green's functions of the localised level, $G_0^{+-}(\omega) \rightarrow D^{++}(\omega)G_0^{+-}(\omega)D^{--}(\omega)$,

so that the diagram is non-zero above the Fermi edge. The time- and anti-time-ordered localised level Green's functions take the form

$$D^{--(++)}(\omega) = \mp \frac{1}{\omega + \Delta \pm i(\alpha_d + \gamma_0^2/2)}.$$

The imaginary part in the denominators reflects the fact

$$n_{>}(\omega) = i \frac{\gamma^2}{2\pi(\alpha_d + \gamma_0^2)} \int_{-\infty}^{\infty} dt e^{i(\omega+\Delta)t} (e^{(\alpha_d+\gamma_0^2)t} \Gamma[t(\alpha_d + \gamma_0^2 + i(\Delta + D))] - e^{-(\alpha_d+\gamma_0^2)t} \Gamma[t(-\alpha_d - \gamma_0^2 + i(\Delta + D))]) \\ \times \int_0^{\infty} d\tau_1 \int_0^{\infty} d\tau_2 e^{i\omega(\tau_1+\tau_2)} \mathcal{K}(\tau_1, 0; t + \tau_1, t + \tau_1 + \tau_2). \quad (85)$$

The asymptotic behaviour of the $n_{>}(\omega)$ close the Fermi edge is not affected (apart from a numerical pre-factor) by the presence of the localised state. There is an important difference – the upper threshold for the TED is now given by Δ instead of D . The reason is that in the presence of the localised state the upper energy limit of the hot hole is given by the energy of the d -level instead of the band-width D (or the applied voltage V).

Thus, in the case of tunnelling via a localised state the TED obtains an additional feature, namely a Lorentzian peak below the Fermi edge, see the inset in Fig. 7. Recent luminescence experiments of Ref. [24] suggest a similar structure – two superimposed peaks in the spectrum of emitted light. The Lorentzian shape of the peaks was probably hidden by the intrinsic Gaussian broadening introduced by the apparatus (a Gaussian fit was adopted in Ref. [24]). The calculation of the emerging luminescence spectra is beyond the scope of this paper and will be discussed elsewhere.

X. SUMMARY AND CONCLUSIONS

In this paper, we studied the energy resolved current (or the TED) emitted from a tip of a correlated host material under out-of-equilibrium conditions. In the uncorrelated case the TED has a sharp threshold at the Fermi edge and there are no particles with energies above it. In the presence of interactions there is a finite high-energy tail due to the hot hole relaxation process. For most systems, the TED is singular right above the Fermi edge.

In the repulsive Luttinger liquid model, where the LDOS is renormalised by interactions and vanishes towards the Fermi edge, the TED below the Fermi edge shows a power-law behaviour with the LDOS exponent. Above the Fermi energy, we also find a power-law but with a new exponent. There is a critical coupling and the TED is divergent for weak interactions but convergent for strong interactions. In the latter case, the TED

that the natural width of the localised level α_d is now widened by the hybridisation with the continuum of states in the host. Using the Fourier transform of the new insertion, which must now be substituted instead of the Fourier transform of $G_0^{+-}(\omega)$ (given in Eq. (15) by $\exp i(\omega - V)t/(t + i\alpha)$), we construct the localised level counterpart of Eq. (15):

has a maximum above the Fermi level. Although the high-energy tail still exists in systems with local interactions confined to the tip, the TED is then a regular function of the energy. Additional features in the TEDs arise in a situation when the tunnelling occurs in two stages via a localised state. In this case there is a Lorentzian peak centred at the energy of this localised level and of the width which depends on the hybridisation with the continuum states on both sides of the contact. All the singularities of the TED above the Fermi energy survive the introduction of the localised level. The singularities in high-energy tails are suppressed as soon as the disorder is introduced. We have calculated the TED of particles tunnelling from a correlated disordered 2D system. In this case the LDOS is exponentially suppressed and this suppression is carried over to the TED. Contrary, in the pure limit, we find a weak (logarithmic) singularity in the TED above the Fermi edge.

We then specialised our results to the case of the FE from carbon nanotubes, both SWNTs and MWNTs. While they are in qualitative agreement with existing experiments, there is little data currently available to test our predictions for the secondary current in these systems. We hope that this work may encourage more measurements, especially at low temperatures ($\ll 300\text{K}$). This could provide additional information about the nature of interactions in nanotubes.

Throughout the paper we consistently worked at zero temperatures. All our results can be generalised to finite temperatures by standard methods (though this may not be of immediate interests until there is more experimental data). There are, of course, other open questions (like the role of higher orders in the tunnelling amplitude) and potentially interesting extensions of this work, which are detailed in the main text.

Also interesting, though more difficult, could be experiments on tunnelling junctions if the TED in such setups were accessible e. g. by means of a tunnel probe [54]. In this case both threshold asymptotics could reveal essen-

tial details about the correlations. Even if direct measurements of the TED are not possible, there is another possibility to identify the secondary effects. Since the hot hole decay is a relaxation process, an electron-hole recombination can occur with an irradiation of a photon. Such a current-driven luminescence effect could be observable in quantum dot systems, where the corresponding experimental techniques became widespread in the recent years [55].

Acknowledgments

We have benefited from illuminating discussions with Nathan Andrei, David Edwards, Reinhold Egger, Fabian Essler, and Yang Chen. This work was supported by the EPSRC of the UK under grants GR/N19359 and GR/R70309. The authors also participate in the EC training network DIENOW.

-
- [1] G. Mahan, *Many-particle physics* (Plenum press, 1991).
- [2] J. W. Gadzuk and E. W. Plummer, *Rev. Mod. Phys.* **45**, 487 (1973).
- [3] J. M. Luttinger, *Phys. Rev.* **119**, 1153 (1960).
- [4] C. Caroli, R. Combescot, P. Nozieres, and D. Saint-James, *J. Phys. C* **4**, 916 (1971).
- [5] A. O. Gogolin and A. Komnik, *Phys. Rev. Lett.* **87**, 256806 (2001).
- [6] C. Lea and R. Gomer, *Phys. Rev. Lett.* **25**, 804 (1970).
- [7] J. W. Gadzuk and E. W. Plummer, *Phys. Rev. Lett.* **26**, 92 (1971).
- [8] R. H. Fowler and L. W. Nordheim, *Proc. Roy. Soc. Lond.* **A119**, 173 (1928).
- [9] L. V. Keldysh, *Zh. Eksp. Teor. Fiz.* **47**, 1515 (1964).
- [10] E. M. Lifshits and L. P. Pitaevskii, *Physical Kinetics* (Pergamon Press, Oxford, 1981).
- [11] C. Dekker, *Phys. Today* **52**, No. 5, 22 (1999).
- [12] R. Egger and A. O. Gogolin, *Phys. Rev. Lett.* **79**, 5082 (1997).
- [13] R. Egger and A. O. Gogolin, *Eur. Phys. J. B* **3**, 281 (1998).
- [14] C. L. Kane, L. Balents, and M. P. A. Fisher, *Phys. Rev. Lett.* **79**, 5086 (1997).
- [15] S. J. Tans, M. H. Devoret, H. Dai, A. Thess, R. E. Smalley, L. J. Geerligs, and C. Dekker, *Nature (London)* **386**, 474 (1997).
- [16] M. Bockrath, D. H. Cobden, J. Lu, A. G. Rinzler, R. E. Smalley, L. Balents, and P. L. McEuen, *Nature (London)* **397**, 598 (1999).
- [17] A. Bachtold, C. Strunk, J. P. Salvetat, J. M. Bonard, L. Forro, T. Nussbaumer, and C. Schönberger, *Nature (London)* **397**, 673 (1999).
- [18] C. Schönberger, A. Bachtold, C. Strunk, J. P. Salvetat, and L. Forro, *Appl. Phys. A* **69**, 283 (1999).
- [19] A. Bachtold, M. de Jonge, K. Grove-Rasmussen, P. L. McEuen, M. Buitelaar, and C. Schönberger, *Phys. Rev. Lett* **87**, 166801 (2001).
- [20] R. Egger and A. O. Gogolin, *Phys. Rev. Lett* **87**, 066401 (2001).
- [21] E. G. Mishchenko, A. V. Andreev, and L. I. Glazman, *Phys. Rev. Lett* **87**, 246801 (2001).
- [22] Q. H. Wang et al., *Appl. Phys. Lett.* **72**, 2912 (1998).
- [23] Y. Saito, *Appl. Phys. A* **67**, 95 (1998).
- [24] J.-M. Bonard, J.-P. Salvetat, et al., *Phys. Rev. Let.* **81**, 1441 (1998).
- [25] V. Meden, C. Wohler, J. Fricke, and K. Schönhammer, *Phys. Rev. B* **52**, 5624 (1995).
- [26] A. A. Abrikosov, L. P. Gorkov, and I. E. Dzyaloshinski, *Methods of quantum field theory in statistical physics* (Dover, New York, 1975).
- [27] M. J. Fransen, T. L. van Rooy, and P. Kruit, *Appl. Surf. Sci.* **146**, 312 (1999).
- [28] M. P. A. Fisher and L. I. Glazman, in *Mesoscopic Electron Transport*, edited by L. Sohn et al. (Kluwer Academic Publishers, 1997).
- [29] S. Tarucha, T. Honda, and T. Saku, *Solid State Commun.* **95**, 413 (1997).
- [30] N. S. Wingreen and Y. Meir, *Phys. Rev. B* **49**, 11040 (1994).
- [31] M. Fabrizio and A. O. Gogolin, *Phys. Rev. B* **50**, 17 732 (1995).
- [32] H. Fröhlich, *Phys. Rev.* **79**, 845 (1950).
- [33] F. D. M. Haldane, *J. Phys. C: Solid State Phys.* **14**, 2585 (1981).
- [34] A. O. Gogolin, A. A. Nersesyan, and A. M. Tsvelik, *Bosonization and Strongly Correlated Systems* (Cambridge University Press, 1998).
- [35] A. Erdélyi, ed., *Higher transcendental functions* (McGraw-Hill, New York, 1953).
- [36] I. Affleck, D. Gepner, H. J. Schulz, and T. Ziman, *J. Phys. A* **22**, 511 (1989).
- [37] P. Benard, L. Chen, and A. M. S. Trembley, *Phys. Rev. B* **47**, 15 217 (1993).
- [38] I. M. Gelfand and G. E. Shilov, *Generalized functions. Vol. 1* (Academic Press, New York, 1964).
- [39] R. Egger, *Phys. Rev. Let.* **83**, 5547 (1999).
- [40] A. M. Finkel'stein, *Zh. Eksp. Teor. Fiz.* **84**, 168 (1983).
- [41] C. Castellani, C. di Castro, P. A. Lee, M. Ma, S. Sorella, and T. Tabet, *Phys. Rev. B* **30**, 1596 (1984).
- [42] D. Belitz and T. R. Kirkpatrick, *Rev. Mod. Phys.* **66**, 261 (1994).
- [43] S. V. Kravchenko, G. V. Kravchenko, J. E. Furneaux, et al., *Phys. Rev. B* **50**, 8039 (1994).
- [44] A. Kamenev and A. Andreev, *Phys. Rev. B* **60**, 2218 (1999).
- [45] M. L. Horbach and G. Schön, *Ann. Physik* **2**, 51 (1993).
- [46] C. Nayak, M. P. A. Fisher, A. W. W. Ludwig, and H. H. Lin, *Phys. Rev. B* **60**, 22 39 (1999).
- [47] J. Rollbühler and H. Grabert, *Phys. Rev. Lett.* **87**, 126804 (2001).
- [48] B. L. Altshuler and A. G. Aronov, *Electron-electron Interactions in Disordered Systems* (Elsevier, Amsterdam, 1985).
- [49] L. Bartosch and P. Kopietz, preprint cond-mat/0108463 (2001).
- [50] L. D. Landau and I. M. Lifshits, *Quantum Mechanics* (Pergamon press, Oxford, 1982).
- [51] F. Ito, K. Konuma, and A. Okamoto, *J. Appl. Phys.* **89**, 8141 (2001).
- [52] J.-M. Bonard, J.-P. Salvetat, et al., *Appl. Phys. A* **69**,

- 245 (1999).
- [53] A. Furusaki and K. A. Matveev, preprint cond-mat/0112426 (2001).
- [54] H. Pothier, S. Guéron, et al., Phys. Rev. Lett. **79**, 3490 (1997).
- [55] E. Dekel, D. Gershoni, et al., Phys. Rev. Lett. **80**, 4991 (1998).